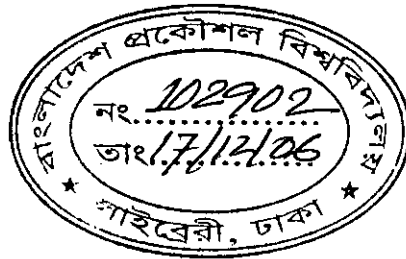


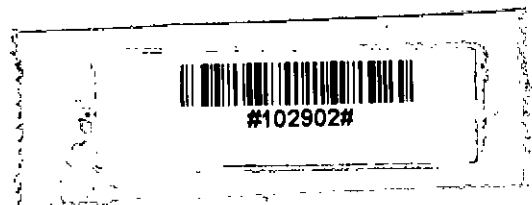
# Development of an Analytical Model of Erbium Doped Silicon Nanocrystal Laser

A thesis submitted to the Department of Electrical and Electronic Engineering  
of  
Bangladesh University of Engineering and Technology  
in partial fulfillment of the requirements for the degree of  
MASTER OF SCIENCE IN ELECTRICAL AND ELECTRONIC ENGINEERING



by


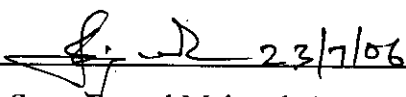

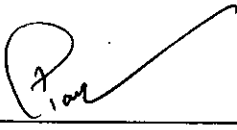
Samia Subrina



DEPARTMENT OF ELECTRICAL AND ELECTRONIC ENGINEERING  
BANGLADESH UNIVERSITY OF ENGINEERING AND TECHNOLOGY  
July 2006

The thesis entitled “**Development of an Analytical Model of Erbium Doped Silicon Nanocrystal Laser**” submitted by Samia Subrina, Roll No.: 040306212P, Session: April 2003, has been accepted as satisfactory in partial fulfillment of the requirements for the degree of MASTER OF SCIENCE IN ELECTRICAL AND ELECTRONIC ENGINEERING on 23 July, 2006.

**BOARD OF EXAMINERS**

1.   
\_\_\_\_\_  
(Dr. Md. Quamrul Huda )  
Professor  
Department of Electrical and Electronic Engineering  
BUET, Dhaka-1000, Bangladesh  
**Chairman**  
(Supervisor)
  
2.   
\_\_\_\_\_  
(Dr. Satya Prasad Majumder)  
Professor and Head  
Department of Electrical and Electronic Engineering  
BUET, Dhaka-1000, Bangladesh  
**Member**  
(Ex-officio)
  
3.   
\_\_\_\_\_  
(Dr. Md. Shafiqul Islam)  
Professor  
Department of Electrical and Electronic Engineering  
BUET, Dhaka-1000, Bangladesh  
**Member**
  
4.   
\_\_\_\_\_  
(Dr. Md. Feroz Alam Khan)  
Associate Professor  
Department of Physics, BUET, Dhaka-1000, Bangladesh  
**Member**  
(External)

# DECLARATION

It is hereby declared that this thesis or any part of it has not been submitted elsewhere for the award of any degree or diploma.

Signature of the Candidate

Samia Subrina

(Samia Subrina)

# **Dedication**

*To my parents*

# Contents

<b>Certification of Thesis</b>	<b>ii</b>
<b>Declaration</b>	<b>iii</b>
<b>Dedication</b>	<b>iv</b>
<b>List of Figures</b>	<b>viii</b>
<b>Acknowledgement</b>	<b>xi</b>
<b>Abstract</b>	<b>xii</b>
<b>1 Introduction</b>	<b>1</b>
1.1 Introduction	1
1.2 Literature Review	2
1.3 Objective of the work	5
1.4 Organization of the thesis	6
<b>2 Erbium luminescence from Silicon and Silicon Nanocrystal</b>	<b>7</b>
2.1 Direct and Indirect Bandgap	7
2.2 Optical properties of Erbium	8
2.3 Nanocrystal Silicon	10
2.4 Excitation Mechanism of Erbium in Nanocrystal Silicon	11
2.5 De-excitation Mechanism of Erbium in Nanocrystal Silicon	13
<b>3 Laser Theory</b>	<b>16</b>
3.1 Emission and absorption of radiation	16
3.2 Einstein relations	18
3.3 Absorption of radiation	19
3.4 Optical feedback	21
3.5 Threshold conditions	21

3.6	Lineshape function	23
3.7	Stimulated emission from Erbium	25
<b>4</b>	<b>Mathematical Model of Erbium Doped Silicon Nanocrystal Laser</b>	<b>26</b>
4.1	Steady state excitation and de-excitation mechanism	26
4.2	Rise time of Erbium luminescence	30
4.3	Decay profile of Erbium luminescence	30
4.4	Stimulated transitions in Erbium doped Nanocrystal Silicon	31
4.5	Condition for LASER action – Threshold	33
4.6	Power vs. Carrier density	34
4.7	Proposed laser device using Erbium doped Nanocrystal Silicon	36
4.7.1	Structure	36
4.7.2	Formulation	38
<b>5</b>	<b>Results and Discussion</b>	<b>40</b>
5.1	Parameters for Erbium incorporated Nanocrystal Silicon	40
5.2	Excited Er atoms and LASER operation	41
5.3	Effects of Different Parameters on Laser Operation	44
5.3.1	Effect of active Erbium concentrations ( $N_{er}$ )	45
5.3.2	Effect of Optical Excitation Source	47
5.3.3	Effect of Internal Loss Coefficient ( $\alpha$ )	48
5.3.4	Effect of Er Radiative Lifetime ( $\tau_{rad}$ )	49
5.3.5	Effect of Spectral Width ( $\Delta\lambda$ )	51
5.3.6	Effect of Input Dependent Loss Coefficient	54
5.4	Time dependent rise of Erbium luminescence	55
5.5	Photoluminescence decay profile	55
5.6	Er doped Bulk Silicon and Nanocrystal Silicon	58
<b>6</b>	<b>Conclusion</b>	<b>63</b>
6.1	Conclusion	63
6.2	Recommendation for future work	64

<b>Bibliography</b>	65
<b>Appendix</b>	69
A Flowchart for calculation of Photoluminescence decay profile of Er atom in nanocrystal Silicon	69

# List of Figures

2.1	E-k diagram for direct and indirect bandgap material	7
2.2	Schematic energy-level diagrams of a free $\text{Er}^{3+}$ ion (left-hand side) and $\text{Er}^{3+}$ in crystal field (right-hand side). Each of the free ion energy levels is split into a manifold of sublevels. (courtesy of Xie. et al. [30])	9
2.3	Cross sectional TEM image of Si/SiO <sub>2</sub> with nc-Si. The presence of nc-Si is evidenced as bright spots in the dark field image. (b) is a detail image of the indicated portion of (a).(courtesy Iacona et al. [27])	10
2.4	PL spectra of SiO <sub>2</sub> films containing nc-Si and Er at room temperature. A broadband at about 1.55eV is due to recombination of excitons in nc-Si and a sharp peak at 0.81eV arises from intra-4f shell transition of $\text{Er}^{3+}$ (courtesy of Fujii et al. [15] )	11
2.5	Photoluminescence spectra measured at 16 K by pumping with a laser of 250 mW three different samples. The Er concentration is $\sim 1 \times 10^{20} \text{ cm}^{-3}$ in all samples. (courtesy of Franzo et al. [17])	12
2.6	Schematic band diagram of Er and nc-Si SiO <sub>2</sub> showing the process of (a) Auger de-excitation (b) Cooperative up-conversion (courtesy of Kik et al. [19])	14
3.1	Diagram illustrating (a) stimulated absorption, (b) spontaneous Emission and (c) stimulated emission. The black dot indicates the electron which takes part in the transition between the two energy levels.	17
3.2	(a) Transmission curve for transitions between two energy levels and (b) emission curve for transition between the energy levels.	24
4.1	Energy level scheme for the system of interacting nc-Si and $\text{Er}^{3+}$ in our proposed model.	27
4.2	Block diagram representation of various transitions in erbium doped nanocrystal silicon laser.	27
4.3	Photon is passing through the cavity medium of gain $k$ . The length of the cavity is $L$ and time for a photon to travel this distance is $\Delta t$ .	33



4.4	Light output and carrier density characteristics of an ideal laser [36]	36
4.5	An optical cavity of the proposed laser.	37
5.1	Excited Er atoms as a function of carrier density with no optical Feedback.	41
5.2	Laser output power as a function of input power to the cavity. The inset shows the photon density per $\text{cm}^3$ as a function carrier density.	42
5.3	Calculated laser output profile under variable pump power to observe the effect of Auger process.	43
5.4	Laser output as a function of pump power to observe the effect of cooperative up-conversion.	44
5.5	Excited erbium atoms as a function of carrier density for different values active Er concentrations, $N_{er}$ .	45
5.6	Pump power dependence of the laser output at $1.54 \mu\text{m}$ for nc-Si samples with different Er concentrations.	46
5.7	Calculated laser output profile under variable pumping with different Energy optical sources. $\text{N}_2$ laser ( $h\nu = 3.7 \text{ eV}$ ) and Ar laser ( $h\nu = 2.5 \text{ eV}$ ) have been used for optical excitation.	47
5.8	Excited erbium atoms as a function of carrier density for different values of loss co-efficient ( $\alpha$ ) with Er concentration of $N_{er} = 10^{20} \text{ cm}^{-3}$ .	48
5.9	Output power vs pump power of Er doped nc-Si laser for different values loss coefficient with $N_{er} = 10^{20} \text{ cm}^{-3}$ .	49
5.10	Excited erbium atom as a function of carrier density for different values of Er radiative lifetime with Er concentration of $N_{er} = 10^{20} \text{ cm}^{-3}$ .	50
5.11	Laser output vs. pump power of Er doped nc-Si laser for different erbium radiative lifetime with Er concentration of $N_{er} = 10^{20} \text{ cm}^{-3}$ . The inset shows only the spontaneous power.	51
5.12	Excited erbium atom as a function of carrier density for different Values of spectral width of emission with Er concentration of $N_{er} = 10^{20} \text{ cm}^{-3}$ .	52

5.13	Excited erbium atom as a function of carrier density for different Values of spectral width of emission with Er concentration of $N_{er} = 6.5 \times 10^{20} \text{ cm}^{-3}$ .	52
5.14	Laser output vs. pump power of Er doped nc-Si laser for different spectral width of emission with Er concentration of $N_{er} = 10^{20} \text{ cm}^{-3}$ .	53
5.15	Effect of input power dependent absorption loss coefficient on the Er doped nc-Si laser output power.	54
5.16	PL intensity profile at two different excitation levels. Both the curves have been normalized to peak values.	55
5.17	PL decay profile at two different excitation levels. Both the curves have been normalized to peak values.	56
5.18	PL intensity profile at 11mW excitation power under two different conditions. Both the curves have been normalized to peak values.	57
5.19	PL intensity profile at 11mW excitation power to observe the impact of cooperative up-conversion effect on PL decay profile while other processes exist in both cases. Both the curves have been normalized to respective peak values.	57
5.20	PL intensity profile at 11mW excitation power to observe the impact of non-radiative processes, except cooperative up-conversion effect, on PL decay profile. The solid line curve shows the decay profile after The inclusion of other non-radiative processes. Both the curves have been normalized to respective peak values.	58
5.21	Photoluminescence Intensity of Er vs. pump power profile. Typical values of different parameters have been used [luminescence from Er:bulk Si system is multiplied by 100].	59
5.22	Calculated PL intensity profile from Erbium doped bulk Silicon under variable photo-excitation. Typical values of different parameters have been used.	60
5.23	Calculated PL intensity profile from Erbium doped nc-Si under variable photo-excitation.	61

# Acknowledgement

The author would like to express her sincere gratitude and profound indebtedness to her thesis supervisor Dr. Md. Quamrul Huda, Professor, Department of Electrical and Electronic Engineering, Bangladesh University of Engineering and Technology (BUET), Dhaka-1000, for his constant guidance, constructive suggestions, commendable support and endless patience through out the progress of this work, without which the work could not have been completed.

Sincere thanks to colleagues and friends for their encouragement and cooperation. Especially the encouraging words from Ms. L. Akter and Mr. Z. Hossain are highly appreciated.

The author would like to thank her parents for their inspiration and patience, which made this thesis come to a fruitful end.

The author is grateful to Bangladesh University of Engineering and Technology, Dhaka-1000, for providing necessary lab facility.

The author is obliged to all officers and staff of the Department of Electrical and Electronic Engineering, BUET, for their cooperation throughout the work.

# ABSTRACT

An analytical model for the erbium excitation and de-excitation processes in nanocrystal silicon (nc-Si) embedded in SiO<sub>2</sub> matrix is developed. The effect of erbium doping into nc-Si is studied. The interaction mechanism of Er ions and silicon nanocrystals is analyzed. The laser cavity is considered to be excited through external optical sources. Recombination rate of photogenerated excitons confined in nc-Si and the subsequent energy transfer to Er<sup>3+</sup> is studied. The expressions of spontaneous and stimulated emission and the stimulated absorption processes are developed in terms of external excitation, erbium concentration etc. The possibility of obtaining laser from Er-doped nanocrystal silicon is investigated and a three level laser model is used for this purpose. Necessary conditions for lasing operation are analyzed and an optical cavity is designed which provides sufficient optical gain to overcome losses and provides useful laser output. The expression for laser output is developed by solving a number of rate equations that involves erbium excitation, photon generation and decay etc. The dependency of laser output on different parameters is studied and good agreement with the characteristics of typical laser is achieved. The effect of enhanced absorption coefficient in higher excitation condition is also incorporated. Numerical simulations of the rate equations are done to observe time dependent behavior of erbium luminescence.

Finally a comparative study on luminescence from erbium, incorporated in bulk and nanocrystal silicon, is performed.



# Chapter One

## Introduction

### 1.1 Introduction

Since the advent of solid state electronics, integrated circuit technology has been growing rapidly. Operating speed of IC chip is increasing with simultaneous increase of the word size. Whenever device speed and chip complexity increase, problems related to interconnection become more and more acute. Interconnection density, interconnect driver limited power dissipation and the system bandwidth are the limiting factors to achieve high speed transmission. These limiting factors also largely affect the increased functionality of integrated circuits. Complete integration of optoelectronic on IC chips can be a viable solution against these present limitations. Under such scheme, data/clock signal is converted by light emitter to optical signal and is transferred to another part of the chip. The optical signal is then decoded by detectors at the receiving end and is converted back to the electrical signal. Optical system offers enormous bandwidth which is suitable for high speed data transmission. Optical transmission is free from any ambient electrical noise, electromagnetic interference, and echoes or cross-talk. Thus optical interconnection offers a high degree of flexibility and versatility.

Silicon is the key element in today's microelectronic industry. Due to mature processing technology and continuous improvement in scale integration, this semiconductor is able to satisfy the increasing demand for higher complexity integrated circuits. If silicon can be realized with optoelectronic components within the single silicon chip, it would extend the functionality of silicon technology from microelectronics to optoelectronic. Several optical functions, such as waveguiding, modulation and optical switching have already been shown to be achievable from silicon [1]. Unfortunately, due to the indirect nature of its energy band structure, silicon is indeed not an efficient light emitter. Achievement of efficient light emission

from crystalline silicon is now being considered as one of the most crucial steps towards the development of fully silicon-based optoelectronic functionality.

The issue of silicon light source is still at an early stage and several different approaches, such as band gap engineering, addition of isovalent impurities or structural defects etc. are being tried to circumvent this drawback. Incorporation of rare earth element erbium into silicon is considered to be one of the most promising approaches in order to obtain efficient light from silicon. The erbium ions, when incorporated in Si exhibit a sharp luminescence at a wavelength of  $\sim 1.54\mu\text{m}$  due to its an intra- $4f$  shell atomic transition between the first excited state  $^4I_{13/2}$  and the ground state  $^4I_{15/2}$ . This wavelength matches to the minimum of the light absorption spectra in silica-based optical fibers. Again, silicon band gap energy is much higher than the photon energy at this wavelength and hence silicon becomes transparent. This avoids the cross-link effect on device performances.

## 1.2 Literature Review

Luminescence from erbium doped silicon was first noticed by Ennen et al. [2] in 1983. They pointed out the potential application of rare earth (RE) element erbium in semiconductor materials, particularly in silicon for the development of light-emitting diodes (LED) and lasers. They showed that the optical transition of erbium in silicon took place between crystal field split-orbit levels  $^4I_{13/2}$  and  $^4I_{15/2}$ . This transition has wavelength around  $1.54\mu\text{m}$  coinciding with the low loss window of standard optical communication. This phenomenon makes the Si:Er system very attractive for silicon based optoelectronics. Klein et al. [3] suggested erbium to be the best suited RE dopant for device application due to its greater lifetime in comparison to other RE elements.

Ennen et al. [4] and Tang et al. [5] carried out photoemission analysis from erbium in silicon. They demonstrated that most of the optically active  $\text{Er}^{3+}$  ions have tetrahedral or lower site symmetries on interstitial lattice sites in Si. Enhancement of luminescence in the presence of impurities such as O, C, N, F or Br has been found by a number of authors. Michel et al. [6] found a large enhancement of luminescence

intensity by introducing oxygen. By using Extended X-ray Absorption Fine Spectroscopy (EXAFS) analysis, Alder et al. [7] found that the impurities modify the chemical surrounding of Er in Si and form erbium impurity complex. Since O activates erbium optically, researches are very much interested in Si:Er system with O co-dopant.

Sharp fall of luminescence intensity with increasing temperature is one of the major limitations of Si:Er system. This phenomenon is called temperature quenching. Libertino et al. [8], showed that only 1% of the total amount of erbium ions introduce a level at 0.15 eV below the silicon conduction band while most of them introduce much shallower level. These shallow levels are hindrance to achieve erbium luminescence at high temperature. Coffa et al. [9] demonstrated that emission of electron from the erbium trap level to the conduction band is responsible for reduced erbium luminescence. Priolo et al. [10] demonstrated that the dissociation of bound excitons results temperature quenching. Kik et al. [11] performed luminescence decay measurement within the temperature range 12 K to 170 K. They observed that the luminescence intensity decreases by the three orders of magnitude as temperature rises from 12 K to 150 K. They pointed out that thermalization of bound excitons and non-radiative energy back transfer process are responsible for temperature quenching. Priolo et al. [12] and Palm et al. [13] also proposed that non-radiative energy back transfer process is the cause of temperature quenching.

Researchers are going through extensive research to overcome this limitation of Er luminescence. Coffa et al. [9] and Priolo et al. [10] demonstrate that co-doping with impurities such as O, C or F reduce temperature quenching significantly. Franzo et al. [14] observed room temperature electroluminescence from Er and O co-doped crystalline p-n Si diodes under both forward and reverse biased conditions and they found that temperature quenching could be significantly reduced while operating under reverse biased condition. Recently, erbium doped silicon nanocrystal has been recognized as a quite efficient method to overcome this problem with increased Er luminescence at room temperature [15-28].

Fujii et al. [15] demonstrated that the modification of the electronic structure provides silicon nanocrystals with functions that do not occur in bulk Silicon. The band structure in nanometer sized silicon becomes more “direct like” in nature and this provides the recombination process more efficient [16].

Franzo et al. [17] demonstrated that the non-radiative de-excitation processes, namely, Auger with free carriers and energy back transfer, limit Er luminescence in bulk crystalline silicon at room temperature, thereby diminishing its potential usefulness in optoelectronics. However, the introduction of  $\text{Er}^{3+}$  ions into nanometer-sized silicon strongly reduces such processes and thereby improves the luminescence yield.

Fujii et al. [18] focused on erbium doped porous Si, which emits strong 1.54  $\mu\text{m}$  luminescence even at room temperature and exhibit very weak temperature quenching of the luminescence. Watanabe carried out photoluminescence analysis from  $\text{SiO}_2$  films containing nc-Si and Er at room temperature. They suggested that the temperature quenching drastically reduced by using Si nanostructures such as porous Si and Si nanocrystals as a host of Er. The band gap widening of Si nanostructures arising from the confinement of electron-hole pair in a small volume (quantum size effect) is considered to be responsible for the observed small temperature quenching [19]. Kenyon et al. [20] pointed out that since optically active erbium ions lie outside the silicon nanocrystals, energy back transfer is suppressed due to presence of an oxide barrier layer between the erbium and the nanocrystal. This also causes weak temperature quenching.

Kik et al. [21] and Priolo et al. [22] experimentally obtained constant Er luminescence upto room temperature. Kik suggested that though nanocrystal decay rate increases with increasing temperature, the energy transfer from nanocrystal to Er occurs within the nanocrystal decay time at room temperature.

Enhancement of luminescence in Er doped nanocrystal silicon has been found by a number of authors [15,18,21,23,26-28]. They argued that the presence of Si nanocrystals in Er doped  $\text{SiO}_2$  considerably enhance the effective Er absorption cross



section because of the large absorption cross section of Si nanocrystals and because of the efficient energy transfer from nanocrystal to erbium ions.

### **1.3 Objective of the Work**

It is now well recognized that erbium (Er) doping of nanocrystal silicon (nc-Si) is an efficient system of obtaining 1.54  $\mu\text{m}$  luminescence at room temperature. Indeed, the excited nc-Si preferentially transfer their energy to the Er ions which subsequently de-excite radiatively. It exhibits very weak temperature quenching of the luminescence and magnifies luminescence intensity since the effective optical cross section of erbium is enhanced due to the presence of nc-Si in Er doped  $\text{SiO}_2$ . Several experimental works have been reported on erbium luminescence in nanocrystal silicon. But a very few work has been reported on stimulated emission of erbium doped nanocrystal silicon.

The objective of this work will be to develop an analytical model for erbium doped nanocrystal silicon laser. The interaction mechanism of Er ions and silicon nanocrystals will be studied. Possibility of laser operation from erbium doped nanocrystal silicon embedded in  $\text{SiO}_2$  matrix will be investigated. Threshold carrier density for lasing will be determined. Laser output versus input power characteristics of Er doped nc-Si laser will be developed from time independent rate equations. Effect of excitation power, erbium concentration, erbium lifetime, loss coefficient etc. on light output will be discussed. At high level of input power, loss coefficient does not remain constant. This effect will be analyzed on light output. Numerical simulations of the rate equations will also be done to observe time dependent behavior of erbium luminescence. Also, efficiency of the Er: nc-Si system with respect to Er: bulk Si system will be studied.

## 1.4 Organization of the Thesis

We know that silicon has very low luminescence efficiency due to its indirect band gap nature. Chapter one describes the necessity of silicon based optoelectronic devices, literature review on erbium doped silicon system and objective of the present work.

Band structure of materials, optical properties of erbium, an overview on silicon nanocrystal and excitation, de-excitation mechanisms of erbium ions incorporated in nanocrystal silicon are given in details in Chapter two.

Chapter three discusses the elementary theory of laser, population inversion, condition of lasing threshold etc.

Mathematical model for erbium doped nanocrystal silicon (nc-Si) laser is developed in chapter four. The erbium luminescence, luminescence rise time and decay time are analyzed mathematically. A laser device is also proposed in this chapter.

Chapter five demonstrates the results for the model equations presented in chapter four. Effects of various parameters are explained with graphical presentation. A comparison between erbium in bulk silicon and that in nanocrystal silicon is analyzed in this chapter.

A brief outlook on these results and recommendations for future works is given in Chapter Six.

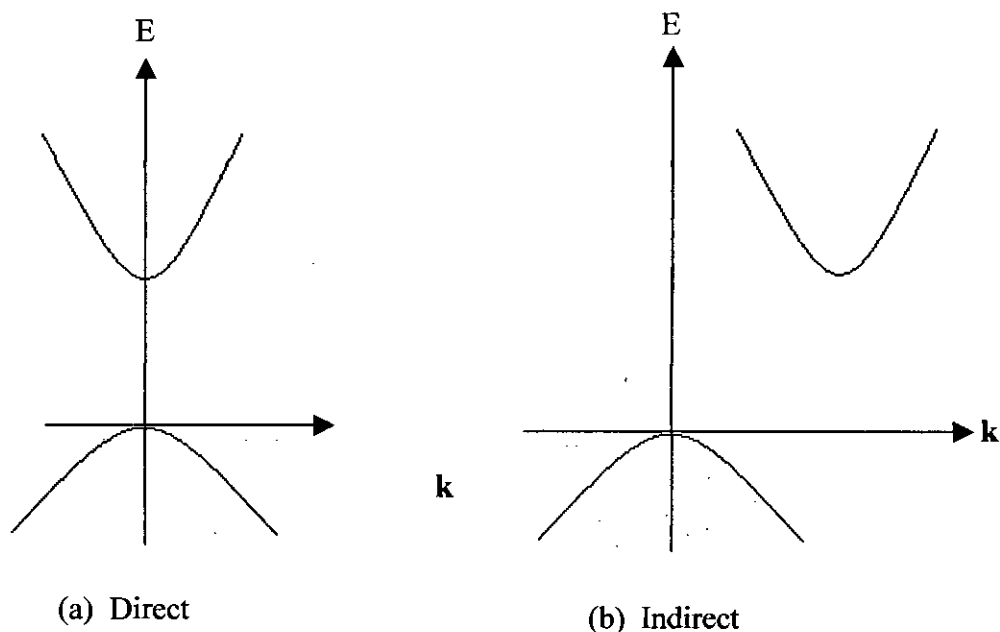
## Chapter Two

# Erbium Luminescence from Silicon and Silicon Nanocrystal

In this chapter, preliminary theory of the luminescence mechanism of erbium doped nanocrystal silicon will be discussed. Direct and indirect bandgap structure, recent works on Er incorporated silicon structure as well as excitation and de-excitation mechanism of erbium atoms in nc-Si will be carried out.

### 2.1 Direct and Indirect Bandgap

Depending on the energy band structure (E-k diagram), crystalline solids are classified into two types: direct bandgap and indirect bandgap material. The energy vs. propagation constant curve (E-k) for two typical cases is shown in Fig. 2.1.



**Fig. 2.1** E-k diagram for direct and indirect bandgap material.

In direct bandgap material, the minimum of the conduction band lies directly above the maximum of the valence band in k-space. Here, an electron at the conduction-

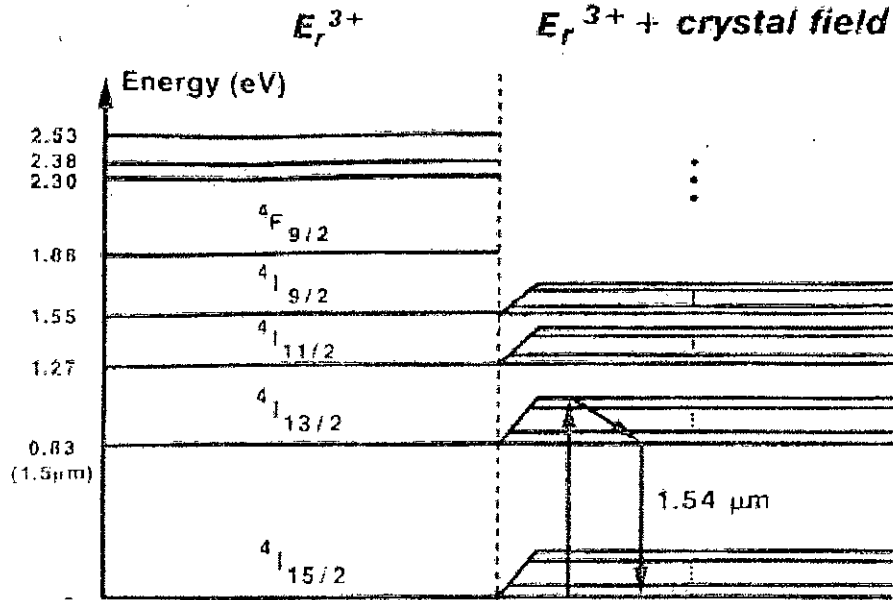
band minimum can recombine directly with a hole at the valence band maximum and conserve momentum. The recombination energy is given up in the form of photons having energy corresponding to bandgap energy. This kind of recombination process is called *radiative recombination* and suitable for light emitting devices. InP, GaAs,  $\text{Al}_x\text{Ga}_{1-x}\text{As}$  etc. are the examples of direct band gap materials.

In indirect bandgap material, the conduction band minimum and valence band maximum have different propagation constant  $k$ . Here direct transition across the bandgap does not conserve momentum and is forbidden. Recombination occurs with the involvement of a third particle like phonon or through a crystallographic defect which allows for the conservation of momentum. The recombination often releases energy as phonons instead of photons. This process is called *non-radiative recombination* and light emission from indirect materials is very inefficient and weak. Examples for indirect material include Si, Ge, and AlAs etc.

Since silicon is the most important semiconductor in today's world, a large effort has been devoted to the realization of silicon based optoelectronic devices. Silicon based optoelectronic technology requires efficient light emission from silicon. But unfortunately due to its indirect bandgap nature, the band-to-band recombination efficiency in silicon is too small for practical uses. Many alternatives are recently investigated and one viable approach is the doping of silicon with erbium.

## 2.2 Optical properties of Erbium

Erbium is a rare earth element belonging to the lanthanide group. It generally has the trivalent charge state  $\text{Er}^{3+}$  when embedded in a solid, losing two electrons from the outermost 6s shell and one electron from the 4f shell and it has then an electronic configuration of  $[\text{Xe}]-4f^{11}$ . The observed transitions from the  $\text{Er}^{3+}$  ions are internal transitions of the 4f states [29]. These transitions are forbidden in case of free ions by the parity selection rule, but are made possible by the crystal field in case of erbium ions in solid. The crystal field intermixes states of opposite parities and splits each



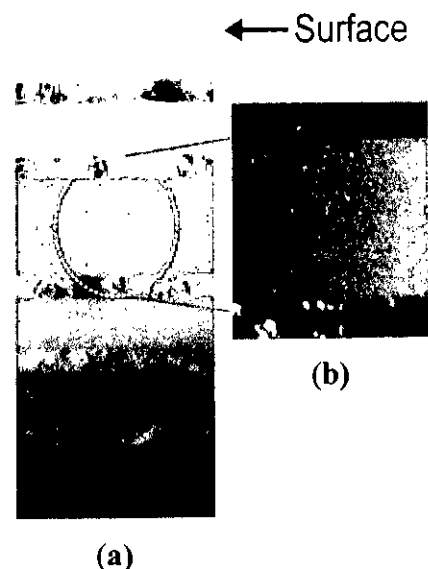
**Fig. 2.2** Schematic energy-level diagrams of a free  $\text{Er}^{3+}$  ion (left-hand side) and  $\text{Er}^{3+}$  in crystal field (right-hand side). Each of the free ion energy levels is split into a manifold of sublevels. (courtesy of Xie, Et al. [30])

single state of a  $\text{Er}^{3+}$  ion into a manifold of sub states with slightly different energies (Fig. 2.2). The transition from the first excited state of  $\text{Er}^{3+}$  ( $4I_{13/2}$ ) to the ground state ( $4I_{15/2}$ ) gives a photon of wavelength  $1.54 \mu\text{m}$  as shown in Fig. 2.2. The luminescence properties are not very sensitive to the host material due to the fact that the  $4f$ -shell is well shielded from its surrounding by  $5s$  and  $5p$  shells. The decay time for the  $1.54 \mu\text{m}$  transition is long which is about a few milliseconds. Once the  $\text{Er}$  is excited to one of its higher levels, it then rapidly decays to the  $4I_{13/2}$  level via multi-phonon emissions. The long decay time of the first excited state  $4I_{13/2}$  provides the possibility of having population inversion and constructing a laser from erbium doped nanocrystal silicon structure. Moreover, the energy difference between the levels is less than the nanocrystal silicon bandgap, making luminescence from erbium feasible in silicon based optoelectronics.

## 2.3 Nanocrystal Silicon

The electronic structure of silicon nanocrystals is strongly modified from that of bulk Si crystals due to the confinement of electrons and holes in a space smaller than the exciton Bohr radius of bulk Si crystals. The modification of the electronic structure provides silicon nanocrystals with functions that do not occur in bulk silicon. The electronic structure changes continuously from the bulk structure with decreasing size. The quantum size effect becomes prominent for nanocrystals smaller than about 10 nm in diameter, and larger nanocrystals can be regarded as bulk from the point of view of electronic structures [15]. Bulk silicon is an indirect bandgap material. Hence lattice vibrations (phonons) are required for the exciton recombination in order to conserve momentum. However, wave functions of quantum confined carriers are spread out in momentum space and the band structure becomes more “direct like” in nature. This provides the recombination process in silicon nanocrystal more efficient [16].

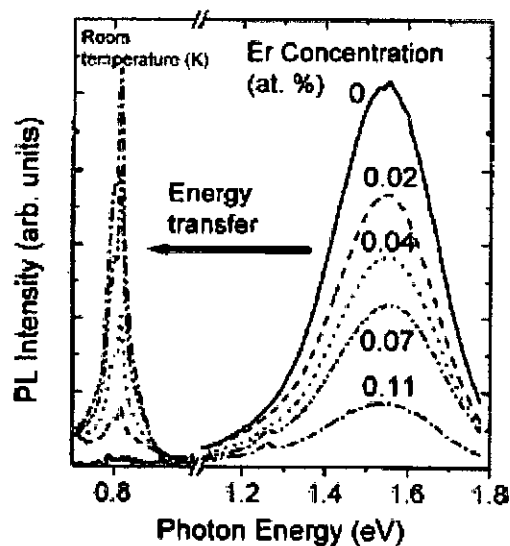
Franzo et al. [17] described that nc-Si were produced by 1250°C annealing of 0.2  $\mu\text{m}$  thick substoichiometric  $\text{SiO}_x$  thin films grown by plasma-enhanced chemical vapor deposition on Si substrates. The size of the nc-Si can be controlled by changing the concentration of silicon or by changing the annealing temperature [15]. As an example a cross sectional transmission electron microscopy (TEM) image of Si/SiO<sub>2</sub> with nc-Si is shown in Fig. 2.3 [27].



**Fig. 2.3** Cross sectional TEM image of Si/SiO<sub>2</sub> with nc-Si. The presence of nc-Si is evidenced as bright spots in the dark field image. (b) is a detail image of the indicated portion of (a). (courtesy Iacona et al. [27])

## 2.4 Excitation Mechanism of Erbium in Nanocrystal Silicon

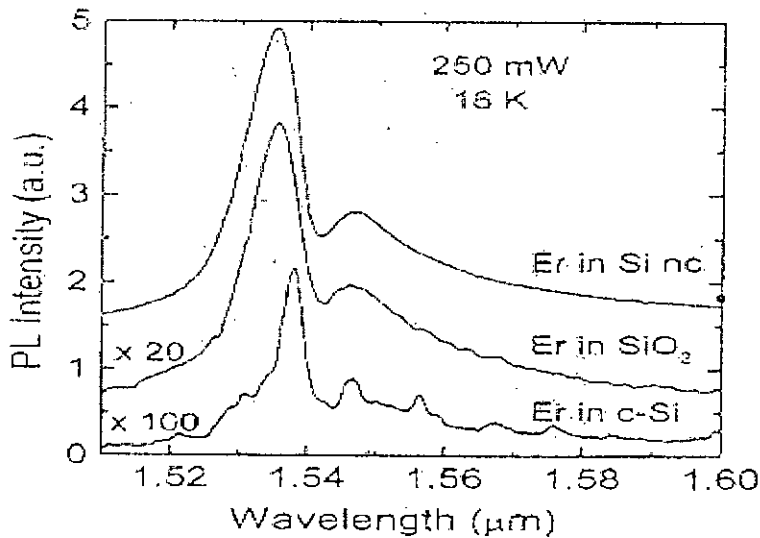
Through extensive research it is now well established that excitation of  $\text{Er}^{3+}$  occurs through the recombination of photogenerated carriers spatially confined in nc-Si and the subsequent energy transfer to  $\text{Er}^{3+}$  [15,17-21,23,26-28]. Franzo et al. [17] demonstrated that the excited nc preferentially transfer their energy to the Er ions which subsequently can de-excite radiatively. They suggested that when Er doped nanocrystal silicon is pumped with an optical source, photons are absorbed by nc-Si and excitons are generated inside the nanocrystals. This exciton, through interfacial state, either recombines radiatively or non-radiatively by bringing Er that is close to the nanocrystal, into one of its excited states. The same excitation model has also been suggested by Kik et al. [21] and Pacifici et al. [26]. Many authors carried out photo emission analysis and observed that the erbium doped nc-Si sample exhibited strong 0.81 eV PL at room temperature as well as 1.5 eV PL due to the recombination of excitons in nc-Si. They found that the 0.81 eV peak becomes strong as the Er concentration increases, while the 1.5 eV peak becomes weak (Fig. 2.4).



**Fig. 2.4** PL spectra of  $\text{SiO}_2$  films containing nc-Si and Er at room temperature. A broadband at about 1.55eV is due to recombination of excitons in nc-Si and a sharp peak at 0.81eV arises from intra-4f shell transition of  $\text{Er}^{3+}$  (courtesy of Fujii et al. [15] )

Considering these results they suggested that erbium ions can be excited efficiently by the energy transfer from nc-Si. Kik et al. [21] also suggested that strong coupling between Si nanocrystal and Er causes intense and stable PL of the  $\text{Er}^{3+}$  ions even at room temperature.

Moreover it is found that due to the small optical cross section for the intra-4f transitions, typically on the order of  $10^{-21} \text{ cm}^2$ , sufficient Er cannot be brought into the first excited state ( $^4\text{I}_{13/2}$ ). On the other hand, because of the large absorption cross section of silicon nanocrystals and because of the efficient energy transfer from nc-Si to  $\text{Er}^{3+}$ , the effective absorption cross section of erbium ions in nc-Si is increased by up to four orders of magnitude. Figure 2.5 reports photoluminescence spectra measured at 16 K by pumping with a 250mW laser beam three different samples: Er + O-implanted crystalline Si (c-Si), Er-implanted  $\text{SiO}_2$ , and Er-implanted nc-Si [17]. It is found that Er-implanted nc-Si luminescence is maximum among all the samples.



**Fig. 2.5** Photoluminescence spectra measured at 16 K by pumping with a laser of 250 mW three different samples. The Er concentration is  $\sim 1 \times 10^{20} \text{ cm}^3$  in all samples. (courtesy of Franzo et al. [17])

The energy transfer to erbium changes with the change of nanocrystal size and causes  $\text{Er}^{3+}$  to excite to one of its energy states. In particular, energy higher than the third excited state of  $\text{Er}^{3+}$  ( $^4\text{I}_{9/2}$ ) is strongly suppressed [16]. From this level, a rapid



relaxation occurs to the  ${}^4I_{11/2}$  level with the subsequent emission of 0.98  $\mu\text{m}$  photons or with a relaxation to the metastable  ${}^4I_{13/2}$  level and emission of photons at 1.54  $\mu\text{m}$ .

## 2.5 De-excitation Mechanism of Erbium in Nanocrystal Silicon

There are two kinds of possible de-excitation mechanisms for the excited erbium atom to come to the ground state ( ${}^4I_{15/2}$ ). The first one is radiative de-excitation and this process is responsible for light emission. The second one is non-radiative de-excitation which does not produce useful light output. Here instead of emitting photons, the energy given up due to transition is wasted away.

The radiative de-excitation between the first excited state ( ${}^4I_{13/2}$ ) and the ground state ( ${}^4I_{15/2}$ ) of  $\text{Er}^{3+}$  ions occurs with a lifetime of approximately 12 ms [19] and emits photon at wavelength of 1.54  $\mu\text{m}$ . This transition level is required in our device and this is the active level where the laser action may take place. Thus to have an efficient luminescence, it is important to suppress the competing non-radiative de-excitation processes which limit the light emission from erbium because of the long decay time of the  ${}^4I_{13/2}$  state.

Depending on the way of de-excitation, non-radiative de-excitation of erbium in silicon nanocrystal includes (i) Auger de-excitation, (ii) Cooperative up-conversion and (iii) others.

**(i) Auger de-excitation:** In this process, excited  $\text{Er}^{3+}$  ion de-excites by giving its energy back to a nearby confined exciton, thus promoting it to a higher energy level (Fig 2.6). After such Auger de-excitation the exciton can relax and subsequently excite an Er ion, effectively bringing the system back to the situation before the exciton was formed. The Auger process in erbium doped nanocrystal silicon, in order to occur, requires a new exciton in nc-Si while an excited Er level is still filled. Hence the effect of Auger process is given by [26],

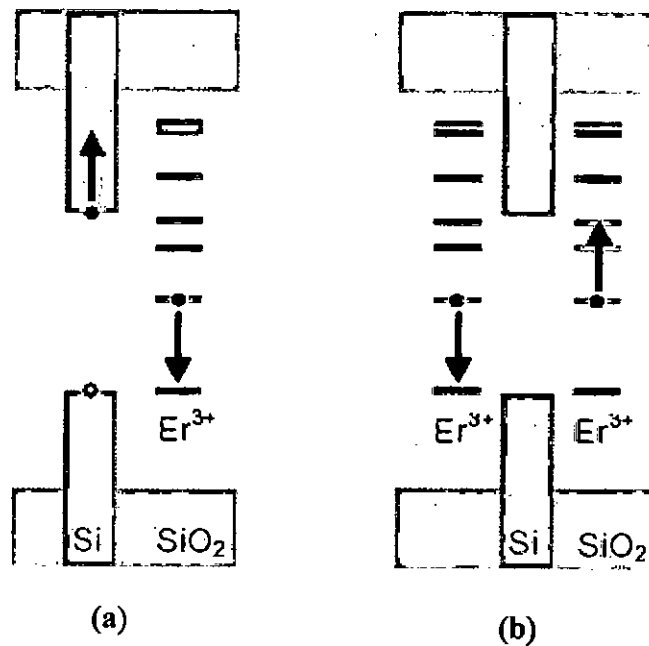
$$C_{\text{A}} n_{\text{Si}} n_{\text{Er}}^*$$

where  $C_{\text{A}}$  is Auger coefficient,  $n_{\text{Si}}$  and  $n_{\text{Er}}^*$  are the excited nc-Si and excited erbium ion concentrations respectively.

(ii) **Cooperative up-conversion:** At sufficiently high Er concentration, two excited Er ions can interact yielding one Er ion in the  $^4I_{9/2}$  state, which rapidly decays to the first excited state, and one Er ion in the ground state (Fig. 2.6). Such process is termed as cooperative up-conversion and causes an important gain limiting effect. This effect lowers the amount of excited Er or conversely, increases the pump power needed to obtain a certain degree of inversion. Cooperative up-conversion is possible due to the presence of a resonant level at twice the energy of the first excited state. The effect of cooperative up-conversion not only depends on the average Er concentration but also on the microscopic distribution of the Er ions on the host material. Cooperative up-conversion effect is given by [26],

$$2C_{up}(n_{er}^*)^2$$

where  $C_{up}$  is cooperative up conversion coefficient and  $n_{er}^*$  is Er concentration in first excited state.



**Fig 2.6** Schematic band diagram of Er and nc-Si SiO<sub>2</sub> showing the process of (a) Auger de-excitation (b) Cooperative up-conversion. (courtesy of Kik et al. [19] )

**(iii) Others:** There exist some other non-radiative decay processes but these are quite inefficient in this system. These processes may include excited state excitation, back transfer mechanism, concentration quenching effect. The impacts of these processes are given by [26],

$$w_{21}n_{er}^*$$

where  $w_{21}$  refers to other non-radiative decay rates and  $n_{er}^*$  is Er concentration in first excited state.

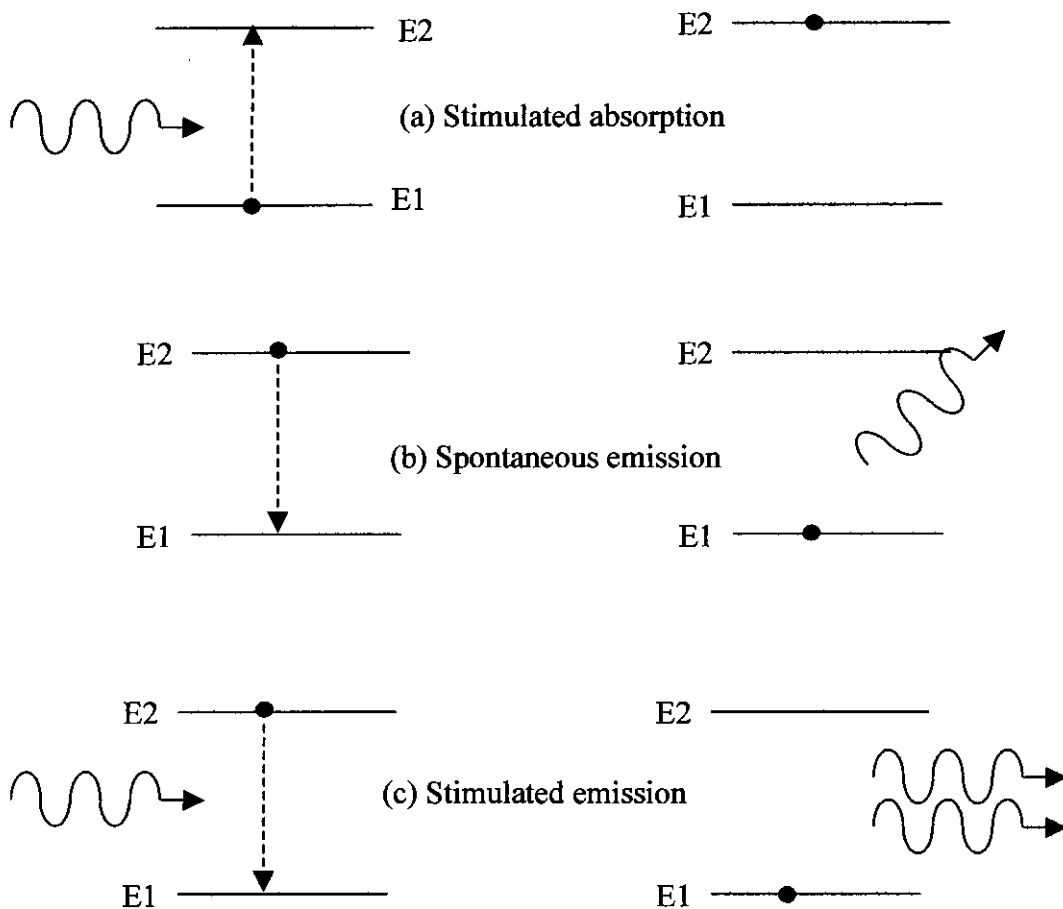
# Chapter Three

## Laser Theory

The word **laser** is an acronym for '*Light Amplification by Stimulated Emission of Radiation*'. A laser is an optical source that emits photons in a coherent beam where the verb *to lase* means "to produce coherent light" or possibly "to cut or otherwise treat with coherent light". The keywords in the discussion of laser theory are stimulated emission and light amplification. In this chapter the concept of stimulated emission, conditions for light amplification and supporting theory will be discussed.

### 3.1 Emission and absorption of radiation

The transition of an electron between two energy states is always accompanied by emission or absorption of a photon. The frequency of emitted or absorbed photon is described by  $\nu = \Delta E/h$  where  $\nu$  is the frequency and  $\Delta E$  is the energy difference between the concerned two levels. If there is an electron in lower energy level  $E_1$  then it may be excited to upper level  $E_2$  by absorbing a photon of energy  $\Delta E = E_2 - E_1$  provided the photon is available. Conversely an electron in upper level may return to lower level by emitting a photon of energy  $\Delta E$ . There are two ways by which the emission can take place. In *spontaneous emission* process the electron drops to lower level in an entirely random fashion. In *stimulated emission* process the transition is initiated by the presence of a photon of right frequency. Figure 3.1 illustrates the absorption and emission processes.



**Fig. 3.1** Diagram illustrating (a) stimulated absorption, (b) spontaneous emission and (c) stimulated emission. The black dot indicates the electron which takes part in the transition between the two energy levels.

Normally the probability of occurrence of spontaneous process is much higher than that of stimulated process. As the spontaneous emission occurs randomly, radiation emitted by large number of atoms by this process is incoherent. But the stimulated emission process results in coherent radiation since the stimulating and stimulated photons have same frequency and same state of polarization and are unidirectional and are in phase. So the amplitude of an incident wave can increase by stimulated emission as it passes through a collection of excited atoms. This is obviously an amplification process of the light wave. The absorption process as the stimulated emission process can occur only in the presence of photons of appropriate energy and hence it is often referred to as *stimulated absorption*.

### 3.2 Einstein relations

If there are  $N_1$  atoms per unit volume in the collection with energy  $E_1$ , then the upward transition rate or absorption rate is proportional to both  $N_1$  and the number of photons of correct frequency, i.e., energy density. So absorption rate is given by  $N_1\rho_\nu B_{12}$  where  $B_{12}$  is a constant and  $\rho_\nu$  is energy density which is given by  $\rho_\nu = N h\nu$ . Here  $N$  is number of photons per unit volume having frequency  $\nu$ . Similarly if there are  $N_2$  atoms per unit volume in the collection with energy  $E_2$ , the stimulated emission rate is given by  $N_2\rho_\nu B_{21}$  where  $B_{21}$  is a constant. The spontaneous emission rate is simply  $N_2 / \tau_{21}$  where  $\tau_{21}$  is the spontaneous lifetime. So the total downward transition rate =  $N_2\rho_\nu B_{21} + N_2/\tau_{21}$ . According to Einstein, for a system in thermal equilibrium the rate of upward transition must be equal to the rate of downward transition. So

$$N_1\rho_\nu B_{12} = N_2\rho_\nu B_{21} + N_2/\tau_{21} \quad (3.2.1)$$

or

$$\rho_\nu = \frac{1/(\tau_{21} B_{21})}{\frac{B_{12} N_1}{B_{21} N_2} - 1} \quad (3.2.2)$$

The populations of various energy levels of a system in thermal equilibrium are given by Boltzmann statistics to be

$$N_j = \frac{g_j N_0 \exp(-E_j/kT)}{\sum g_i \exp(-E_i/kT)} \quad (3.2.3)$$

where  $N_j$  is the population density of the energy level  $E_j$ ,  $N_0$  is the total population density and  $g_j$  is the degeneracy of the  $j$ th level. So

$$\frac{N_1}{N_2} = \frac{g_1}{g_2} \exp((E_2 - E_1)/kT) \quad (3.2.4)$$

Therefore substituting equation (3.2.4) in equation (3.2.2)

$$\rho_\nu = \frac{1/(\tau_{21} B_{21})}{\frac{B_{12} g_1}{B_{21} g_2} \exp(h\nu/kT) - 1} \quad (3.2.5)$$

Since the collection of atoms in the system is in thermal equilibrium it must give rise to radiation which is identical to blackbody radiation. So the radiation density can be described by

$$\rho_\nu = \frac{8\pi h\nu^3}{c^3} \frac{1}{\exp(h\nu/kT)-1} \quad (3.2.6)$$

Comparing equations (3.2.5) and (3.2.6)

$$g_1 B_{12} = g_2 B_{21} \quad (3.2.7)$$

and

$$\frac{1/\tau_{21}}{B_{21}} = \frac{8\pi h\nu^3}{c^3} \quad (3.2.8)$$

Equations (3.2.7) and (3.2.8) are called *Einstein relations*. The ratio  $g_1/g_2$  is generally in the order of unity and hence ignored. Thus taking refractive index of the medium into account we get

$$B_{12} = B_{21} = \frac{c^3}{8\pi h \tau_{21} \nu^3 n^3} \quad (3.2.9)$$

where  $n$  is the refractive index of the medium.

From the above discussion it is clear that stimulated emission process competes with spontaneous emission and absorption process. In order to amplify a beam of light by stimulated emission, the rate of this process must be increased. This can be done by increasing both  $N_2$  and  $\rho_\nu$ .

### 3.3 Absorption of radiation

Let us consider a collimated beam of perfectly monochromatic radiation of unit cross sectional area passing through an absorbing medium. We assume that there is only one relevant electron transition which occurs between the energy levels  $E_1$  and  $E_2$ . The change in irradiance of the beam as a function of distance is given by

$$\Delta I(x) = I(x+\Delta x) - I(x)$$

For a homogeneous medium  $\Delta I(x)$  is proportional to both the distance traveled and to  $I(x)$ . That is  $\Delta I(x) = -\delta I(x)\Delta x$ . The proportionality constant  $\delta$  is called *absorption coefficient*. The negative sign indicates the reduction in beam irradiance due to absorption, as  $\delta$  is a positive quantity. Writing this expression as a differential equation we get

$$\frac{dI(x)}{dx} = -\delta I(x)$$

Integrating this equation we have

$$I = I_0 \exp(-\delta x) \quad (3.3.1)$$

where  $I_0$  is the incident irradiance

So, due to absorption the irradiance decreases exponentially with distance. If we can make  $\delta$  negative then  $(-\delta x)$  in the exponent of equation (3.3.1) becomes positive. So the beam irradiance grows as it propagates through the medium in accordance with the equation

$$I = I_0 \exp(kx) \quad (3.3.2)$$

where  $k = -\delta$  is called the *small signal gain coefficient*. It can be shown that the expression of  $\delta$  is given by [36]

$$\delta = \left( \frac{g_2}{g_1} N_1 - N_2 \right) \frac{B_{21} h \nu n}{c} \quad (3.3.3)$$

where  $n$  is the refractive index of the medium. So the expression of  $k$  is given by

$$k = \left( N_2 - \frac{g_2}{g_1} N_1 \right) \frac{B_{21} h \nu n}{c} \quad (3.3.4)$$

In order to make  $k$  positive  $N_2$  must be greater than  $\frac{g_2}{g_1} N_1$ . As normally  $\frac{g_2}{g_1} \cong 1$  then condition for beam amplification is  $N_2 > N_1$ . As  $E_2$  is the upper energy level, normally population density in energy level  $E_2$  is lower than that of  $E_1$ . So in order to get amplification, we need to create a non-equilibrium distribution of atoms among various energy levels of the atomic system. The non-equilibrium condition is called *population inversion*. In order to create population inversion a large amount of energy



must be supplied to excite atoms to upper energy level. This excitation process is called *pumping*.

### **3.4 Optical feedback**

Laser is more analogous to an oscillator than an amplifier. In an electronic oscillator, an amplifier tuned to a particular frequency is provided with positive feedback. When switched on, electrical noise signal of appropriate frequency appearing at the input will be amplified. The amplified output is fed back to the input and further amplified and so on. A stable output is quickly reached since the amplifier saturates at high input voltages. In laser, positive feedback is obtained by placing the gain medium between a pair of mirrors which form an optical cavity. The initial stimulus is provided by any spontaneous transition between appropriate energy levels in which the emitted photon travels along the axis of the system. The signal is amplified as it passes through the medium and fed back by the mirrors. Saturation is reached when gain provided by the medium exactly matches the losses incurred during a complete round trip.

The gain per unit length of most active media is so small that very little amplification of a beam of light results from a single pass through the medium. But in the multiple passes, which a beam undergoes when the medium is placed within a cavity, the amplification may be substantial.

### **3.5 Threshold conditions**

A steady state level of oscillation is reached when the rate of amplification is balanced by the rate of loss. This is the situation in continuous output lasers. In pulse laser the situation is little different. While population inversion is a necessary condition for laser action, it is not sufficient because the gain coefficient must be large enough to overcome the losses and sustain oscillations. The total loss of the system is due to a number of different processes such as

1. Transmission at the mirrors - the transmission from one of the mirrors usually

provides the useful output, the other mirror is made as reflective as possible to minimize losses.

2. Absorption and scattering at the mirrors.
3. Absorption in the laser medium due to undesired transitions.
4. Scattering at optical inhomogeneities in the laser medium.
5. Diffraction losses at the mirrors.

Let us include all the losses except those due to transmission at the mirrors in a single effective loss coefficient  $\alpha$ , which reduces the effective gain coefficient to  $k-\alpha$ . We can determine the threshold gain by considering the change in irradiance of a beam of light undergoing a round trip within the laser cavity. Let us assume that the laser medium is placed between the mirrors  $M_1$  and  $M_2$ , which have reflectances  $R_1$  and  $R_2$  and a separation  $L$ . Then in traveling from  $M_1$  to  $M_2$  the beam irradiance increases from  $I_0$  to  $I$  where

$$I = I_0 \exp(k-\alpha)L$$

After reflection at  $M_2$ , the beam irradiance will be  $R_2 I_0 \exp(k-\alpha)L$  and after a complete round trip the final irradiance will be  $R_1 R_2 I_0 \exp\{2(k-\alpha)L\}$ . The ratio of final to initial irradiance is given by

$$G = \frac{\text{Final irradiance}}{\text{Initial irradiance}} = R_1 R_2 \exp\{2(k-\alpha)L\}$$

If  $G$  is greater than unity a disturbance at the laser resonant frequency will undergo a net amplification and the oscillations will grow. If  $G$  is less than unity the oscillations will die out. Therefore we can write the threshold condition as

$$G = R_1 R_2 \exp\{2(k_{th}-\alpha)L\} = 1 \quad (3.5.1)$$

where  $k_{th}$  is the threshold gain. It is important to realize that the threshold gain is equal to the steady state gain in continuous output lasers, i.e.  $k_{th} = k_{ss}$ . This equity is due to a phenomenon known as *gain saturation*. In terms of population inversion there will be a threshold value  $N_{th} = [N_2 - (g_2/g_1) N_1]_{th}$  corresponding to  $k_{th}$ . In steady state condition  $[N_2 - (g_2/g_1) N_1]$  remains equal to  $N_{th}$  regardless of the amount by which the threshold pumping rate is exceeded. The small signal gain coefficient at

threshold can be obtained from equation (3.5.1).

$$k_{th} = \alpha + \frac{1}{2L} \ln\left(\frac{1}{R_1 R_2}\right) \quad (3.5.2)$$

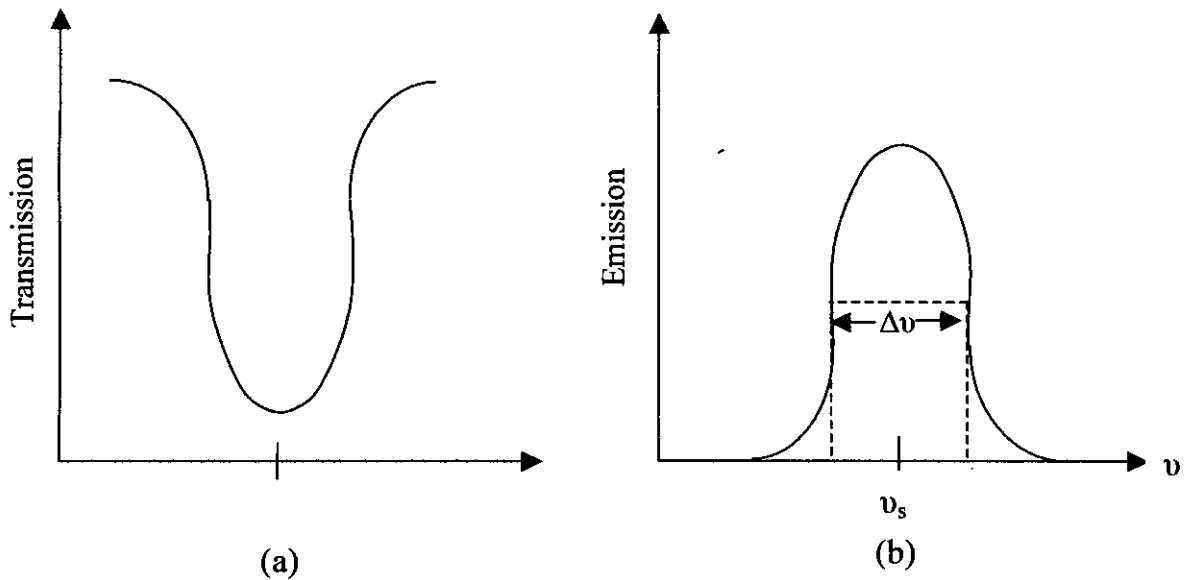
where the first term represents the volume losses and the second the loss in the form of useful output. The value of  $k_{th}$  can also be found from equation (3.3.4) as

$$\begin{aligned} k_{th} &= \left( N_2 - \frac{g_2}{g_1} N_1 \right)_{th} \frac{B_{21} h \nu n}{c} \\ &= N_{th} \frac{B_{21} h \nu n}{c} \end{aligned} \quad (3.5.3)$$

Equations (3.5.2) and (3.5.3) show that  $k$  can have a wide range of values depending not only on  $[N_2 - (g_2/g_1) N_1]$  but also on intrinsic properties of the active medium.

### 3.6 Lineshape function

So far we have assumed that all the atoms would be able to interact with the perfectly monochromatic beam. In fact this is not so. Spectral lines have a finite wavelength spread. This can be seen in both emission and absorption and if we are to measure transmission as a function of frequency for the transition between the two energy levels  $E$  and  $E_2$  we would obtain the bell-shape curve shown in Figure 3.2(a). The emission curve would be the inverse of this (have shown in Figure 3.2(b)).



**Fig. 3.2** (a) Transmission curve for transitions between two energy levels and (b) emission curve for transition between the energy levels.

The shape of these curves is described by *line shape function*  $g(\nu)$ .  $g(\nu)$  can also be used to describe a frequency probability curve.  $g(\nu) d\nu$  may be defined as the emission or absorption of a photon whose frequency lies between  $\nu$  and  $\nu + d\nu$ .  $g(\nu)$  is normalized such that  $\int_{-\infty}^{\infty} g(\nu) d\nu = 1$ . Therefore a photon of energy  $h\nu$  may not necessarily stimulate another of energy  $h\nu$ .  $g(\nu)d\nu$  can be taken as the probability that the stimulated photon will have an energy between  $h\nu$  and  $h(\nu + d\nu)$ . When a monochromatic beam of frequency  $\nu_s$  interacts with a group of atoms with a lineshape function  $g(\nu)$ , the small signal gain coefficient may be written as [36].

$$k(\nu_s) = \left( N_2 - \frac{g_2}{g_1} N_1 \right)_{th} \frac{B_{21} h \nu_s n g(\nu_s)}{c} \quad (3.6.1)$$

It can be shown that  $g(\nu_s) = \frac{1}{\Delta\nu}$ , where  $\nu_s$  is the frequency at which the value of the function is maximum and  $\Delta\nu$  is the linewidth, i.e., the separation between two points on the curve where the function falls to half of its peak value which occurs at  $\nu_s$ . The form of the line shape function  $g(\nu)$  depends on the particular mechanism responsible for *spectral broadening* in a given transition.

### 3.7 Stimulated emission from Erbium

As mentioned before, emission at 1.54  $\mu\text{m}$  wavelength can be obtained from Er doped nc-Si due to internal 4f shell transition of excited Er atoms from  $^4I_{13/2}$  to  $^4I_{15/2}$ . By optical excitation, a large number of electrons are supplied to the conduction band of nc-Si. These electrons will recombine with holes of valence band via interfacial state Si=O and the recombination energy will excite Er atoms to first excited state ( $^4I_{13/2}$ ). From this state a fraction of excited atoms will return to ground state ( $^4I_{15/2}$ ) radiatively giving rise to emission of photons (spontaneous emission). The photons will stimulate the generation of more photons and soon laser oscillations will build up inside the cavity. Useful output may be obtained through one of the mirrors used in the cavity.

# Chapter Four

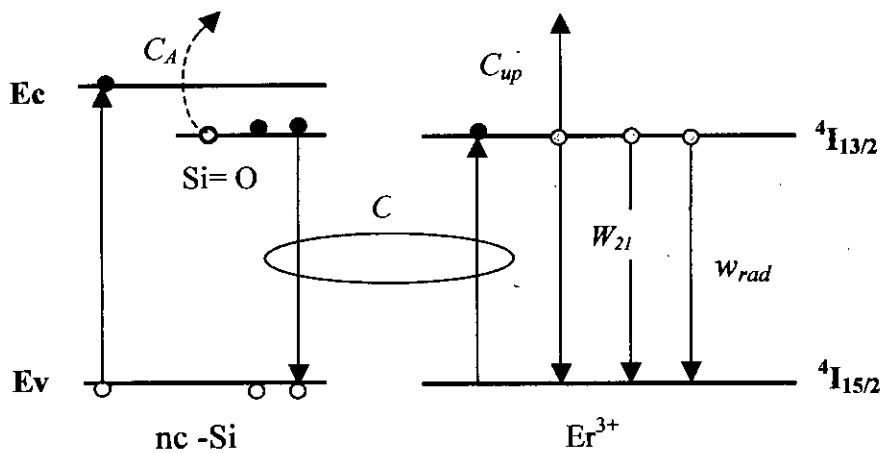
## Mathematical Model of Erbium Doped Silicon Nanocrystal Laser

In this chapter the mathematical model for excitation and de-excitation of Er atoms in nc-Si embedded in SiO<sub>2</sub> will be presented. Equations for pumping and decay will be described for both steady state and time varying case. The model will include stimulated emission and absorption in steady state. Necessary conditions for lasing operation will be analyzed. A practical laser using Er doped nc-Si will be proposed and the expression for its output power will be obtained.

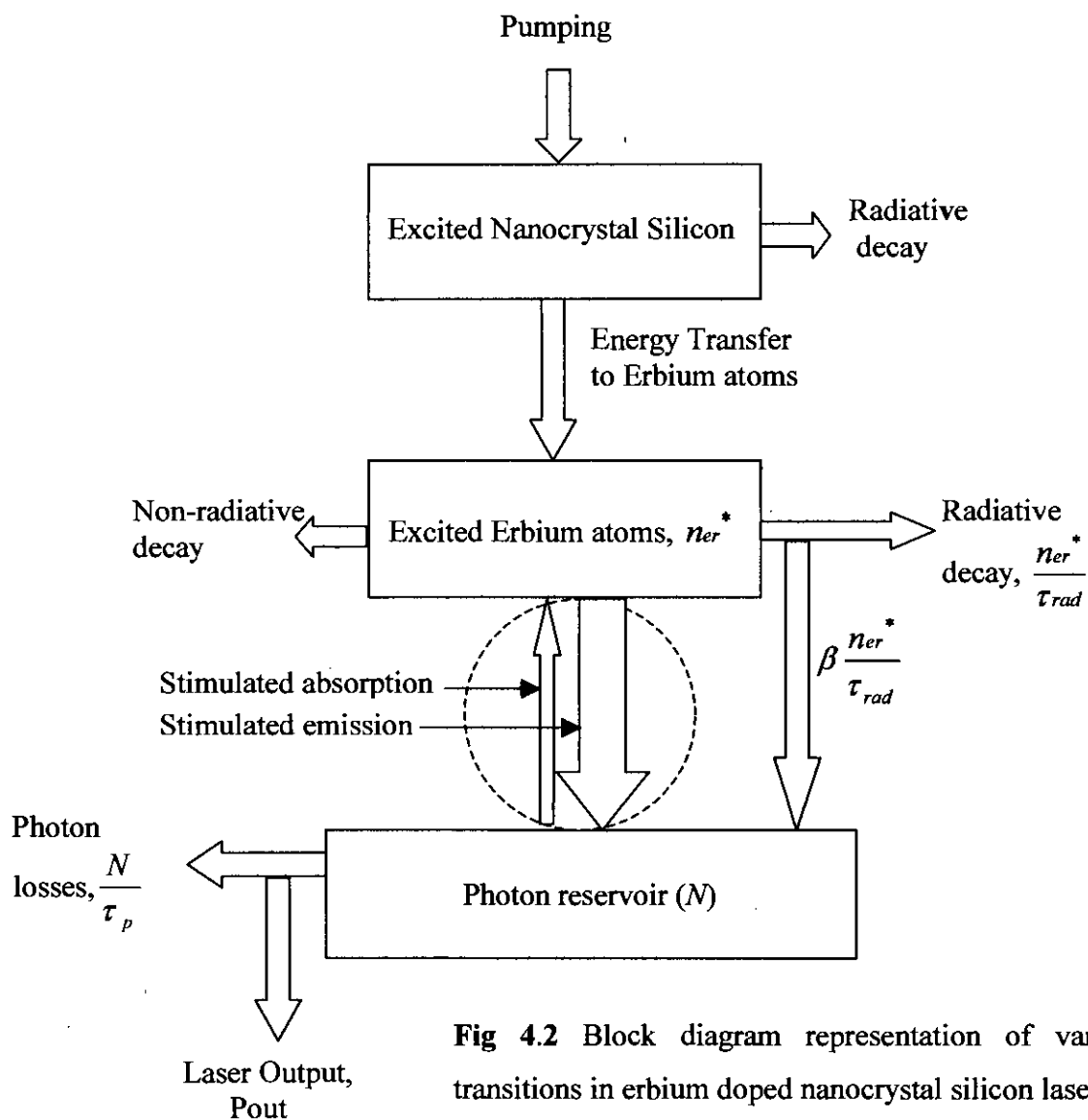
### 4.1 Steady state excitation and de-excitation mechanism

It is analyzed that when Er doped nanocrystal silicon is pumped with an optical source, photons are absorbed by the nc-Si and promote an electron from the conduction band to the valence band. The electron in the conduction band is then trapped by a Si=O interface state [17]. The recombination of electron in the interfacial state with a hole in the valence band emits a photon with an energy that depends on the nanocrystal size. Alternatively, in presence of Er, the energy can be transferred to the Er ion to bring erbium into one of its excited state.

Since the 0.8  $\mu\text{m}$  nc wavelength (corresponding to 1.5 eV with a 1.6 nm sized nc-Si) couples well with the  $^4I_{9/2}$  level of the Er manifold, we propose that this is indeed the Er level first excited by the nanocrystal. From this level, a rapid relaxation occurs to the  $^4I_{11/2}$  level and then to the metastable  $^4I_{13/2}$  level and emission of photons at 1.54  $\mu\text{m}$ .  $^4I_{13/2}$  is the most long-lived level as compared to other Er levels [26]. This helps us to consider the Er as a three levels system. Figs. 4.1 and 4.2 represent the models used to develop the rate equations and the expression for laser output.



**Fig 4.1** Energy level scheme for the system of interacting nc-Si and Er<sup>3+</sup> in our proposed model.



**Fig 4.2** Block diagram representation of various transitions in erbium doped nanocrystal silicon laser.

Let,

$N_{ER}$  = total number of erbium atoms per unit volume.

$n_{er}^*$  = total number of excited erbium atoms at steady state per unit volume.

$C$  = coupling coefficients, which describes the coupling between the excited nc-Si and ground state of Er,  $\text{cm}^3\text{-s}^{-1}$

$n_{si}$  = carrier density in nanocrystal silicon at steady state per unit volume.

In erbium doped nanocrystal silicon, Er is excited through an electron-hole mediated process. It is suggested that Er ions, responsible for strong luminescence, are located in  $\text{SiO}_2$  or at the Si/ $\text{SiO}_2$  interface. But, if an Er atom is already in the excited state due to previous recombination of electron-hole pair, the recombination energy will be wasted away.

So Let,

$N_{er}$  = total number of active erbium atoms per unit volume.

$N_{er} - n_{er}^*$  = number of active erbium atoms available for excitation at steady state per unit volume.

At steady state, pumping rate or excitation rate from the ground state ( $^4I_{15/2}$ ) to the first excited state ( $^4I_{13/2}$ ) per unit volume per second is given by

$$P = Cn_{si}(N_{er} - n_{er}^*) \quad (4.1.1)$$

Once excited, the Er atom can de-excite from  $^4I_{13/2}$  to the ground state either radiatively or non-radiatively. If the radiative decay lifetime is  $\tau_{rad}$  then the radiative decay rate per unit volume per second is given by

$$\begin{aligned} \text{Decay rate (radiative)} &= \frac{n_{er}^*}{\tau_{rad}} \\ &= W_{rad}n_{er}^* \end{aligned} \quad (4.1.2)$$

On the other hand, the competing parallel non-radiative decay process includes Auger de-excitation with nearby excitons, Cooperative up conversion and others.



The Auger de-excitation in erbium doped nanocrystal silicon, in order to occur, requires a new exciton in nc-Si while an excited Er level is still filled. Hence the effect of Auger process is given by,

$$C_{ANsi}n_{er}^* \quad (4.1.3)$$

where  $C_A$  is Auger coefficient in  $\text{cm}^3\text{-s}^{-1}$ .

Cooperative up conversion effect is given by

$$2C_{up}(n_{er}^*)^2 \quad (4.1.4)$$

where  $C_{up}$  is cooperative up conversion coefficient in  $\text{cm}^3\text{-s}^{-1}$

Thus the de-excitation rate, at steady state, per unit volume per second is given by

$$D = (w_{21} + w_{rad})n_{er}^* + 2C_{up}(n_{er}^*)^2 + C_{ANsi}n_{er}^* \quad (4.1.5)$$

where  $w_{21}$  refers to non-radiative decay rates, other than Auger and cooperative up conversion processes, in  $\text{sec}^{-1}$ .

At steady state, the rate of excitation and de-excitation must be equal.

$$Cn_{si}(N_{er} - n_{er}^*) = (w_{21} + w_{rad})n_{er}^* + 2C_{up}(n_{er}^*)^2 + C_{ANsi}n_{er}^* \quad (4.1.6)$$

So at steady state the number of excited Er atoms per unit volume is given by

$$n_{er}^* = \frac{-(Cn_{si} + C_{ANsi} + w_{21} + w_{rad}) + \sqrt{(Cn_{si} + C_{ANsi} + w_{21} + w_{rad})^2 + 8C_{up}Cn_{si}N_{er}}}{2C_{up}} \quad (4.1.7)$$

The luminescence strength is given by

$$I \propto \frac{n_{er}^*}{\tau_{rad}} \quad (4.1.8)$$

## 4.2 Rise time of Erbium luminescence

When a laser pulse is applied to an Er doped nc-Si, excitons in nc-Si are generated instantly, which transfer the recombination energy to Er atoms through strong coupling mechanism. Rise time of erbium luminescence to the steady state (after providing a laser excitation power) can be obtained from the corresponding time dependent Er luminescence by solving rate equations of excited erbium sites. The Er atoms are excited at faster rate just after the excitation. After sometime, excitation rate becomes equal with de-excitation rate and finally erbium luminescence gets to steady value during the external excitation.

The excitation and de-excitation rates, in this case, are time dependent. The excitation rate is  $Cn_{si}(N_{er}-n_{er}^*(t))$  and similarly the de-excitation rate is  $[(w_{21}+w_{rad})n_{er}^*(t)+C_A n_{si} n_{er}^*(t)+2Cup(n_{er}^*(t))^2]$ . So increase in number of excited Er atoms per second, i.e., the rate of change of excited Er is given by

$$\frac{dn_{er}^*(t)}{dt} = Cn_{si}(N_{er}-n_{er}^*(t)) - [(w_{21}+w_{rad})n_{er}^*(t) + C_A n_{si} n_{er}^*(t) + 2Cup(n_{er}^*(t))^2] \quad (4.2.1)$$

The exact analytical solution of this differential equation will be complicated. So numerical solution of the differential equation using fourth order Runge-Kutta method with an initial condition of  $n_{er}^*(0) = 0$  will be obtained.

## 4.3 Decay profile of Erbium luminescence

When the external excitation pulse on an erbium doped specimen is switched off, the number of excited erbium states starts decreasing from the steady state. The strength of erbium luminescence gradually decays to zero. Hence to find out the time dependent luminescence, the rate equation of excited Er atoms is to be solved. In this case, both the number of excited Er atoms and carrier concentrations are functions of time.

The rate of change of excited Er atoms is given by

$$\frac{dn_{er}^*(t)}{dt} = Cn_{si}(t)(N_{er} - n_{er}^*(t)) - [(w_{21} + w_{rad})n_{er}^*(t) + C_A n_{si}(t)n_{er}^*(t) + 2C_{up}(n_{er}^*(t))^2] \quad (4.3.1)$$

Here  $n_{si}(t)$  is time dependent carrier concentrations. Whenever the laser pulse is switched off, optically generated carrier concentration starts to decrease exponentially. If  $n_{si}$  is the optically generated concentration at steady state condition then  $n_{si}(t)$  is given by

$$n_{si}(t) = n_{si} e^{-t/\tau_{si}}$$

where  $\tau_{si}$  = life time of carrier.

Since both excited Er and carrier concentrations are time varying functions, analytical solution of equation (4.3.1) is a complex one. So numerical solution techniques (fourth order RK method) will be employed (flowchart is given in Appendix). The steady state condition prior to termination of laser pulse will be used as initial value of  $n_{er}^*$ .

#### 4.4 Stimulated transitions in Erbium doped Nanocrystal Silicon

So far our study was concerned with the Er luminescence through spontaneous emission. In order to incorporate stimulated emission and absorption, the rate equations have to be modified.

The stimulated absorption or excitation rate is proportional to unexcited Er concentration and energy density.

$$\text{So stimulated excitation rate} = (N_{er} - n_{er}^*)\rho_{\nu}B_{12}$$

where  $B_{12}$  is a constant and  $\rho_{\nu}$  is energy density which is given by  $\rho_{\nu} = N h\nu$ .  $N$  is the number of photons per unit volume having frequency  $\nu$ .

The stimulated emission or de-excitation rate is proportional to excited Er concentration and energy density.

$$\text{Hence stimulated de-excitation rate} = n_{er}^* \rho_v B_{21}$$

where  $B_{21}$  is a constant.

So considering both spontaneous and stimulated transitions, the modified rate equations are:

$$\text{excitation rate} = C_{nsi}(N_{er} - n_{er}^*) + (N_{er} - n_{er}^*) \rho_v B_{12} \quad (4.4.1)$$

$$\text{de-excitation rate} = (w_{21} + w_{rad})n_{er}^* + 2C_{up}(n_{er}^*)^2 + C_{Ansi}n_{er}^* + n_{er}^* \rho_v B_{21} \quad (4.4.2)$$

Since at steady state, these two rates must be equal. So

$$C_{nsi}(N_{er} - n_{er}^*) + (N_{er} - n_{er}^*) \rho_v B_{12} = (w_{21} + w_{rad})n_{er}^* + 2C_{up}(n_{er}^*)^2 + C_{Ansi}n_{er}^* + n_{er}^* \rho_v B_{21} \quad (4.4.3)$$

The photon density i.e. energy density,  $\rho_v$  is increased by the stimulated emission and by the fraction  $\beta$  of spontaneously emitted photons that enter into the lasing mode. The factor  $\beta$  is usually very small ( $\sim 10^{-4}$ ) and spontaneous emission can often be neglected above threshold. The photon density  $N$  is reduced from the cavity by internal absorption and scattering losses ( $\alpha_i$ ) and also by emission through end mirrors ( $\alpha_m$ ). These photon losses are characterized by the photon life time  $\tau_p$  where

$$1/\tau_p = v_g (\alpha_i + \alpha_m) \quad (4.4.4)$$

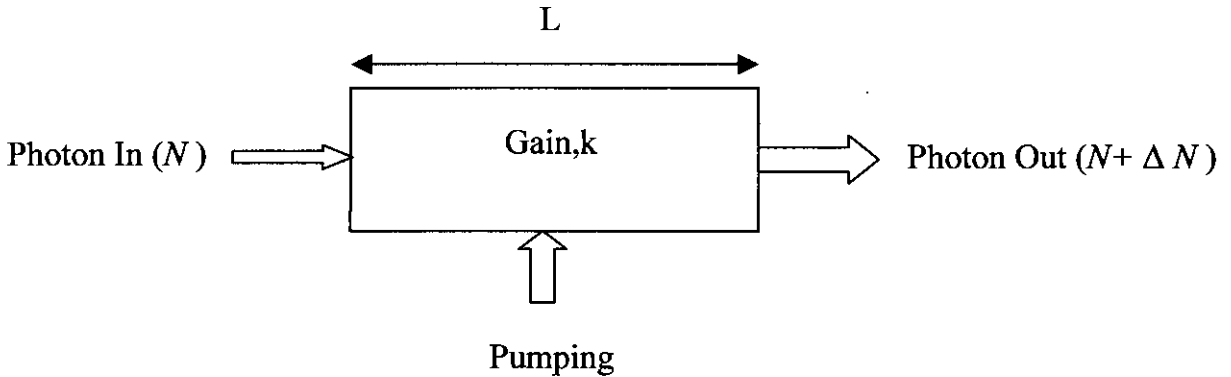
$v_g$  is the velocity of light inside the cavity and  $v_g = c/n_r$  where  $c$  is the free space light speed and  $n_r$  is the refractive index of the cavity [37].

Therefore the rate of change of photons per unit volume can be written as

$$\begin{aligned} \frac{dN}{dt} &= n_{er}^* \rho_v B_{21} + \beta \frac{n_{er}^*}{\tau_{rad}} - (N_{er} - n_{er}^*) \rho_v B_{12} - \frac{\rho_v}{h\nu \tau_p} \\ &= (2n_{er}^* - N_{er}) \rho_v B_{21} + \beta \frac{n_{er}^*}{\tau_{rad}} - \frac{N}{\tau_p} \end{aligned} \quad (4.4.5)$$

considering  $B_{12} = B_{21}$

This is a gain process of photons if stimulated emission dominates the stimulated absorption otherwise it is a loss process.



**Fig. 4.3** Photon is passing through the cavity medium of gain  $k$ . The length of the cavity is  $L$  and time for a photon to travel this distance is  $\Delta t$ .

#### 4.5 Condition for LASER action – Threshold

Below the threshold level, the value of  $\rho_0$  can be neglected, as lasing has not yet occurred and most of the pump power appears as spontaneous transitions. So equation (4.1.6) can be used instead of equation (4.4.3) in order to obtain the rate equations below threshold. Thus using equation (4.1.6), the number of excited Er atoms in the absence of any optical feedback in the cavity is given by

$$n_{er}^* = \frac{-(Cn_{si} + CAn_{si} + w_{21} + w_{rad}) + \sqrt{(Cn_{si} + CAn_{si} + w_{21} + w_{rad})^2 + 8C_{up}Cn_{si}N_{er}}}{2C_{up}}$$

But when stimulated transition occurs, the excited Er atoms clamp to its threshold level  $n_{erth}^*$ . The gain of the cavity medium also depends upon the excited Er atom. So, when threshold occurs, gain also becomes constant at its threshold value  $k_{th}$ . At this condition, there is a balance between gain and optical loss in the cavity.

At threshold,  $\rho_0$  is still small and equation (4.1.6) can be used to obtain the expression of carrier density at threshold condition. Thus

$$Cn_{si\_th}(N_{er} - n_{erth}^*) = (w_{21} + w_{rad})n_{erth}^* + 2C_{up}(n_{erth}^*)^2 + CAn_{si\_th}n_{erth}^*$$

$$\Rightarrow n_{si\_th}(C(N_{er} - n_{er}^*) - C_{A}n_{er}^*) = (w_{21} + w_{rad})n_{er}^* + 2C_{up}n_{er}^{*2}$$

$$\Rightarrow n_{si\_th} = \frac{(w_{21} + w_{rad})n_{er}^* + 2C_{up}n_{er}^{*2}}{C(N_{er} - n_{er}^*) - C_{A}n_{er}^*} \quad (4.5.1)$$

where  $n_{si\_th}$  = carrier density at threshold.

## 4.6 Power vs. Carrier density

The optical output power is proportional to the photon density, which is given by [37]

$$\text{Output power, } P_{out} = \left( \begin{array}{c} \text{Energy of} \\ \text{a photon} \end{array} \right) \times \left( \begin{array}{c} \text{Photon} \\ \text{density} \end{array} \right) \times \left( \begin{array}{c} \text{Cavity} \\ \text{volume} \end{array} \right) \times \left( \begin{array}{c} \text{Escape rate} \\ \text{of a photon} \end{array} \right) \quad (4.6.1)$$

The energy of a photon is  $h\nu$ . If the mirror loss term is  $\alpha_m$ , then escape rate of the photons through the mirrors is  $v_g \alpha_m$ . So the output power emitted through both mirrors is given by

$$P_{out} = h\nu N(Vol^m) v_g \alpha_m \quad (4.6.2)$$

### Condition (i): Below Threshold

Below the threshold level, very low intensity light is generated due to spontaneous emission. Neglecting the stimulated transition term from Eq. (4.4.5), at steady state we get,

$$N_{sp} = \beta \frac{\tau_p}{\tau_{rad}} n_{er}^* \quad (n_{si} < n_{si\_th}) \quad (4.6.3)$$

This is the photon density inside the cavity due to spontaneous emission. From Eq. (4.1.7) we get,

$$n_{er}^* = \frac{-(Cn_{si} + C_{A}n_{si} + w_{21} + w_{rad}) + \sqrt{(Cn_{si} + C_{A}n_{si} + w_{21} + w_{rad})^2 + 8C_{up}Cn_{si}N_{er}}}{2C_{up}}$$

From Eqs. (4.6.2) and (4.6.3) we get the spontaneous emission power,

$$P_{sp} = h\nu \left( \beta \frac{\tau_p}{\tau_{rad}} n_{er}^* \right) (Vol^m) v_g \alpha_m \quad (4.6.4)$$

It is clear that the photon generated during spontaneous transition depends upon the excited Er atoms. At threshold, the spontaneous emission clamps as the excited erbium atoms  $n_{er}^*$  clamp to its threshold value  $n_{erth}^*$ . Thus, as the carrier density is increased above threshold ( $n_{si} > n_{si\_th}$ ), the spontaneous power remains constant at the value with  $n_{si} = n_{si\_th}$ .

### Condition (ii): Above Threshold

Since above the threshold level ( $n_{si} > n_{si\_th}$ ), the excited erbium atoms  $n_{er}^*$  becomes fixed to its threshold value  $n_{erth}^*$ , so from Eq. (4.4.3) the expression of  $\rho_v$  at steady state can be written as

$$\rho_v = \frac{Cn_{si}(N_{er} - n_{erth}^*) - (w_{21} + w_{rad})n_{erth}^* - 2Cup(n_{erth}^*)^2 - CAn_{si}n_{erth}^*}{B_{21}(2n_{erth}^* - N_{er})} \quad (4.6.5)$$

Hence the photon density inside the cavity due to stimulated emission is given by

$$N_{st} = \frac{\rho_v}{h\nu}$$

Thus the photon density inside the cavity in the lasing mode, where both spontaneous and stimulated transitions occurs is given by

$$N = N_{sp} + N_{st}$$

But above the threshold level, the stimulated emission plays the dominant role over spontaneous emission. Infact spontaneously emitted photons are needed to trigger lasing initially but most of these photons do not contribute to the laser beam. Hence it can be considered that above threshold  $N \approx N_{st}$ . From Eq.(4.6.5), we found that if the input power is increased, the number of carrier ( $n_{si}$ ) will increase which will increase the non-radiative decay rate (namely Auger effect).So above threshold the only parameters, in the expression of photon density, dependent on input power are  $n_{si}$  and non-radiative decay rate.

So the laser output power after threshold is

$$\begin{aligned}
 P_{out} &= N * h\nu * v_g * \alpha_m * Vol && (n_{si} > n_{si\_th}) \\
 &= \rho_v * v_g * \alpha_m * Vol && (4.6.6)
 \end{aligned}$$

Eq. (4.6.6) represents the total output power of both mirrors.

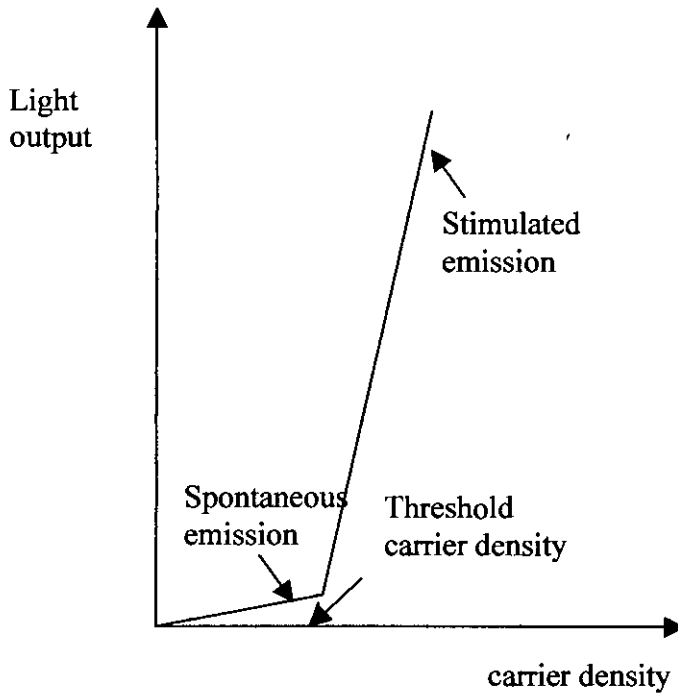


Fig. 4.4 Light output and carrier density characteristics of an ideal laser [36]

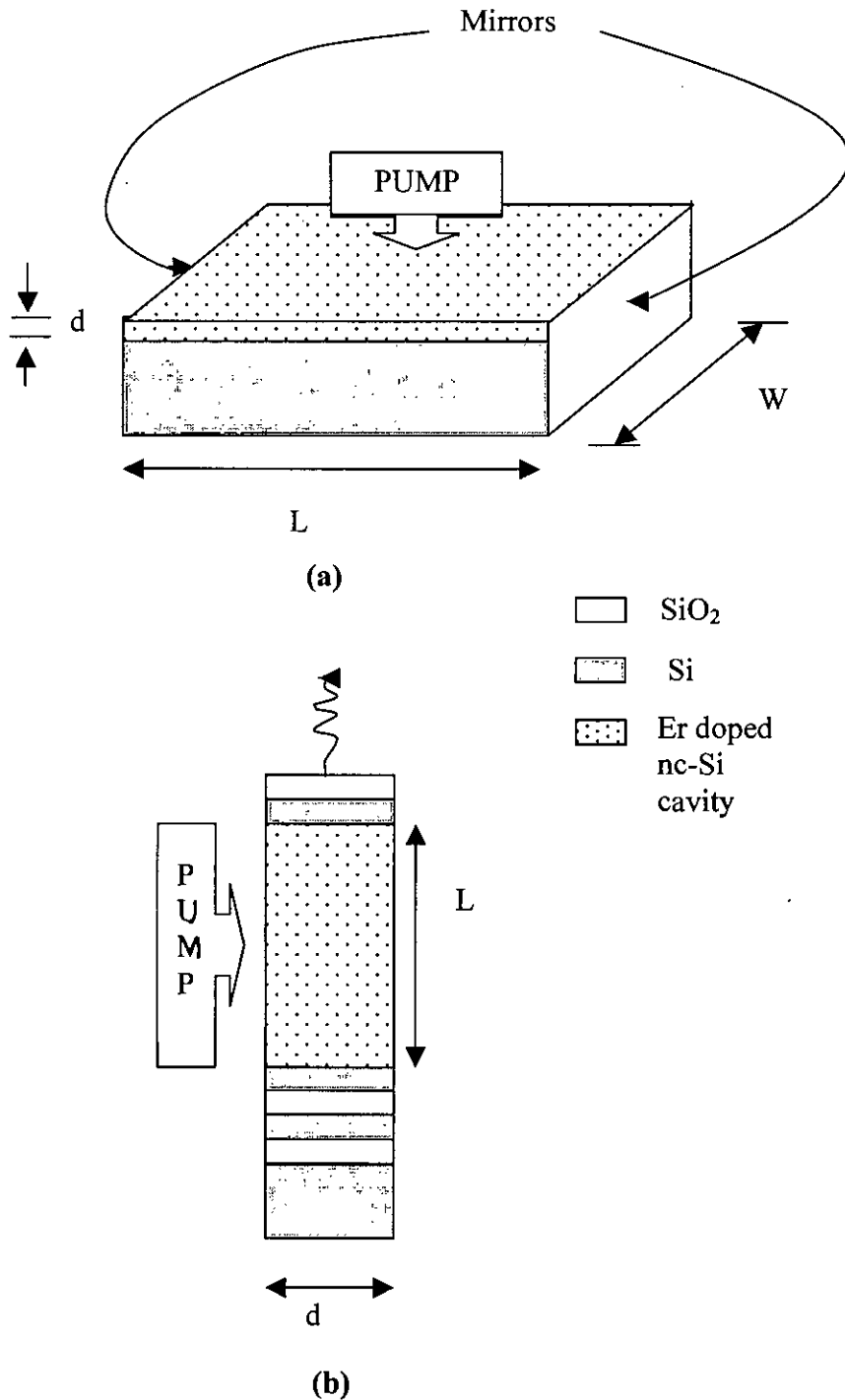
## 4.7 Proposed laser device using Erbium doped Nanocrystal Silicon

### 4.7.1 Structure

A practical laser cavity may be constructed using SiO<sub>2</sub> films containing nc-Si and Er, prepared by co-sputtering method. When the sample is optically excited, a photon is absorbed by the nanocrystal, which causes generation of an exciton inside the nanocrystal. This photogenerated exciton can recombine non-radiatively by bringing Er into one of its excited state as it is assumed that there is a strong coupling between Si nanocrystal and Er. A fraction of these excited Er atoms decay radiatively



producing photons of fixed frequency. These photons can interact with excited and unexcited Er atoms giving rise to stimulated emission and absorption. If the photo-generated carrier concentration becomes large enough, the stimulated emission can exceed the absorption so that optical gain can be achieved. When the round trip gain will exceed the total loss over the same distance, laser oscillation will occur.



**Fig 4.5** An optical cavity of the proposed laser.

Mirrors of the cavity can be cleaved flat edge (Fig 4.5(a)) or distributed Si/SiO<sub>2</sub> bragg reflectors (Fig 4.5(b)). In case of bragg reflectors, spectral width can be controlled by changing the number of Si/SiO<sub>2</sub> layers.

#### 4.7.2 Formulation

In order to find out the contribution of optical excitation to carrier concentrations in conduction band and valence band of nc-Si, it is required to calculate the optical generation rate first. If 100% absorption efficiency is assumed then optical generation rate is given by

$$g_{op} = \frac{P/V}{h\nu} \quad \text{per cm}^3 \text{ per sec}$$

and the optically generated carrier concentration

$$n_{op} = g_{op} \times \tau_{si} = \frac{P/V}{h\nu} \times \tau_{si} \quad \text{per cm}^3 \quad (4.7.2.1)$$

where

$P$  = total cavity power supplied by laser, watt

$V$  = volume of the cavity, cm<sup>3</sup>

$\tau_{si}$  = lifetime of the nanocrystal silicon, sec

$h$  = plank's constant, J-s

$\nu$  = frequency of photon, Hz

Optical excitation is made through laser with certain spot diameter and penetration depth (usually of the order of 1  $\mu\text{m}$ ). Since practical laser cavity usually provides depth of the order of 1  $\mu\text{m}$ , so it is possible to excite all the possible nanocrystals through proper excitation mechanism.

Let,

$A$  = cross sectional area of the cavity,

$a$  = effective optical cross section of a nanocrystal silicon

$N_{si}$  = total number of nc-Si per cm<sup>3</sup>

Total number of nc-Si in the laser cavity =  $N_{si} \times V$

So, effective optical cross section of nanocrystal silicons =  $a \times (N_{si} \times V)$  cm<sup>2</sup>

Ratio of effective cross section of nc-Si to cavity =  $\frac{a \times (N_{si} \times V)}{A}$

Effective carrier concentration,

$$\begin{aligned} n_{si} &= n_{op} \times \frac{a \times (N_{si} \times V)}{A} \\ &= \frac{P/V}{h\nu} \times \tau_{si} \times \frac{a \times (N_{si} \times V)}{A} \text{ per cm}^3 \end{aligned} \quad (4.7.2.2)$$

# Chapter Five

## Results and Discussion

The mathematical expressions to illustrate the various characteristics of erbium doped nanocrystal silicon laser have been derived in the previous chapter. A computer program is developed based on these derived equations to generate numerical data. The analysis has been done for both steady state and time varying conditions of spontaneous emission and for steady state stimulated transitions. In this chapter results of these analysis, their significance and the effect of various parameters on Er luminescence and laser output will be discussed.

### 5.1 Parameters for Erbium incorporated Nanocrystal Silicon

Throughout the analysis, our proposed laser cavity is characterized by:

Volume =  $300\mu\text{m} \times 300\mu\text{m} \times 1\mu\text{m}$ ; Mirror reflectivities are  $R_1=R_2=90\%$ .

For optical excitation, 488 nm line of  $\text{Ar}^+$  laser having a spot diameter of 3 mm and penetration depth of 1  $\mu\text{m}$  have been used.

Values of different parameters used are,

$$\tau_{rad} = 12\text{ms as stated in Kik et al. [19]}$$

$$C = 3 \times 10^{-15} \text{ cm}^3 \text{ s}^{-1} \text{ as proposed in Pacifici et al. [26]}$$

$$C_A = 2.9 \times 10^{-19} \text{ cm}^3 \text{ s}^{-1} \text{ [26]}$$

$$C_{up} = 7 \times 10^{-17} \text{ cm}^3 \text{ s}^{-1} \text{ [26]}$$

$$w_{21} = 420 \text{ s}^{-1} \text{ [26]}$$

$$\tau_{si} = 21\mu\text{s as stated in Kik et al. [21]}$$

$$\text{effective optical cross section of 1.6 nm nc-Si, } a = 5 \times 10^{-16} \text{ cm}^2$$

as stated in Franzo et al. [17]

Unless otherwise specified the following values have been used for calculation of our analysis:

$$\text{effective number of nc-si per unit volume, } N_{si} = 10^{19} \text{ per cm}^3$$

effective number of Er atom per unit volume,  $N_{er} = 10^{20}$  per  $\text{cm}^3$

all the observations have been carried out at room temperature.

Parameters used to calculate the threshold value of population inversion are:

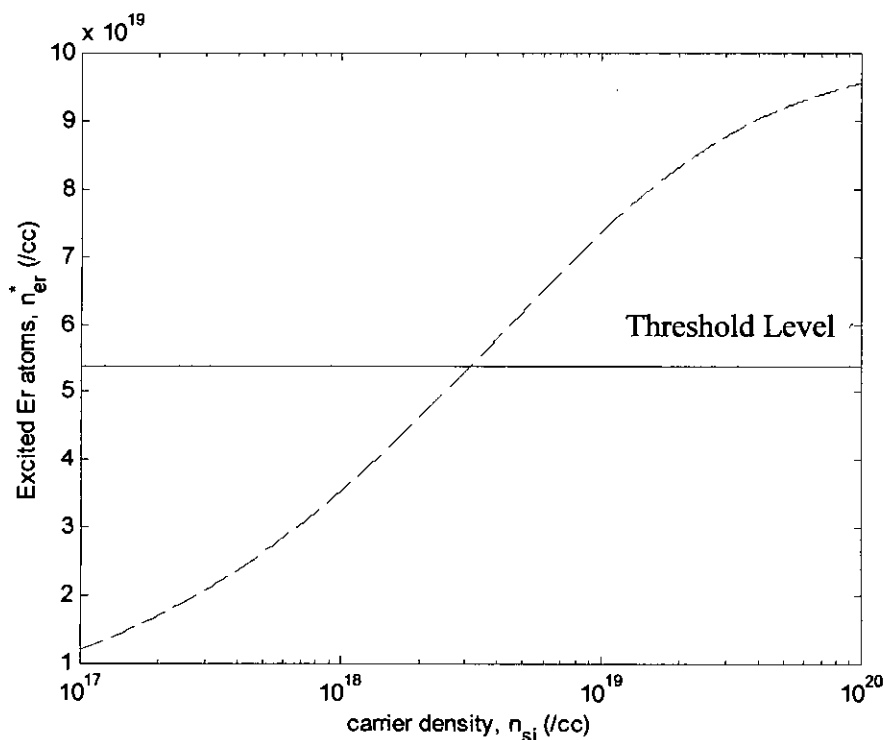
loss coefficient,  $\alpha = 20 \text{ cm}^{-1}$

free-space wavelength  $\lambda = 1.54 \text{ }\mu\text{m}$

$\Delta\lambda$  corresponding to  $\Delta\nu = 1 \text{ }\text{\AA}$

refractive index of the cavity medium,  $n_r = 1.44$

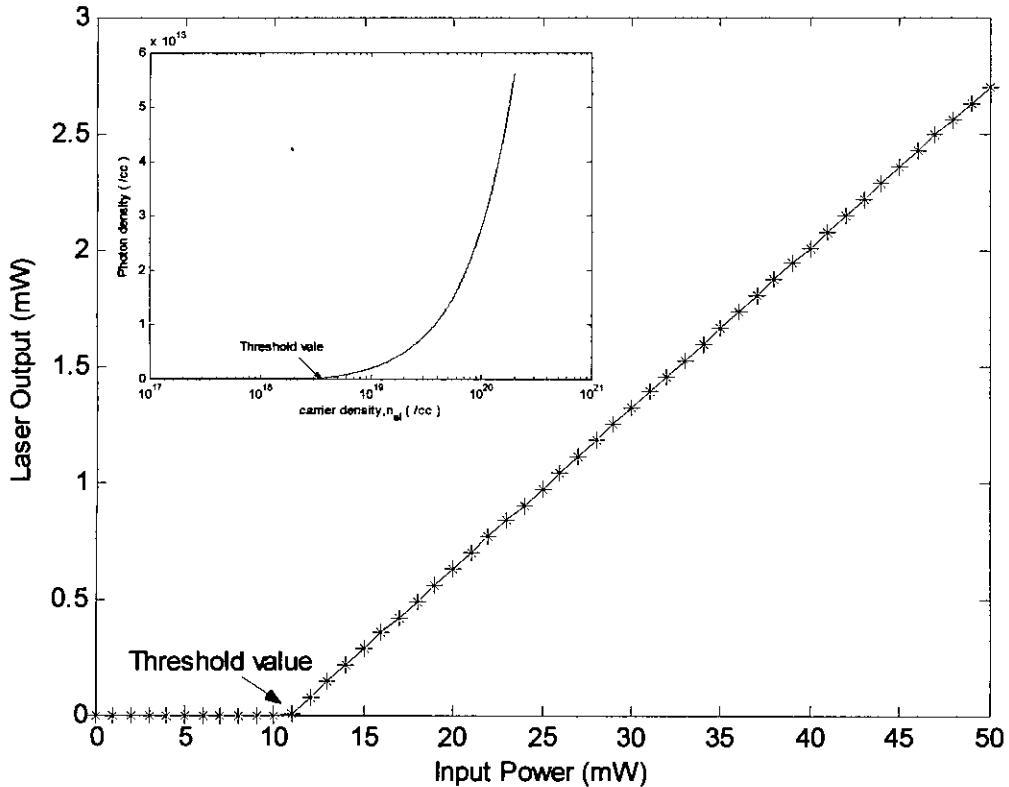
## 5.2 Excited Er atoms and LASER operation



**Fig. 5.1** Excited Er atoms as a function of carrier density with no optical feedback

In this section, we have investigated how much amount of erbium atoms can be excited from the ground level to the  $^4I_{13/2}$  state in the absence of any optical feedback for our proposed device. We have also calculated the threshold value of population inversion, hence the threshold value of excited erbium atoms, for the lasing condition using Eq. (3.6.1). At this point the gain exactly equals the cavity losses. From this, if

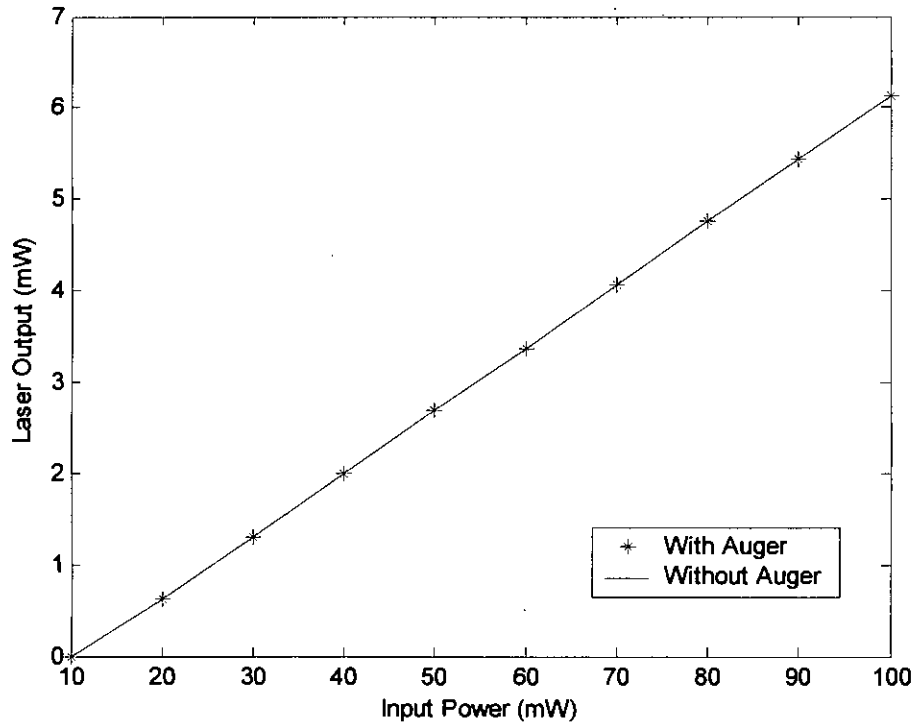
the amount of erbium atoms in the excited state exceeds this threshold level, laser operation is possible. But when lasing occurs, the excited erbium atoms clamps to its threshold value due to stimulated transition and further increase of population inversion with excitation is impossible in a steady state condition. From Fig (5.1), it is clear that laser operation is possible with our proposed device.



**Fig 5.2** Laser output power as a function of input power to the cavity. The inset shows the photon density per  $\text{cm}^3$  as a function carrier density.

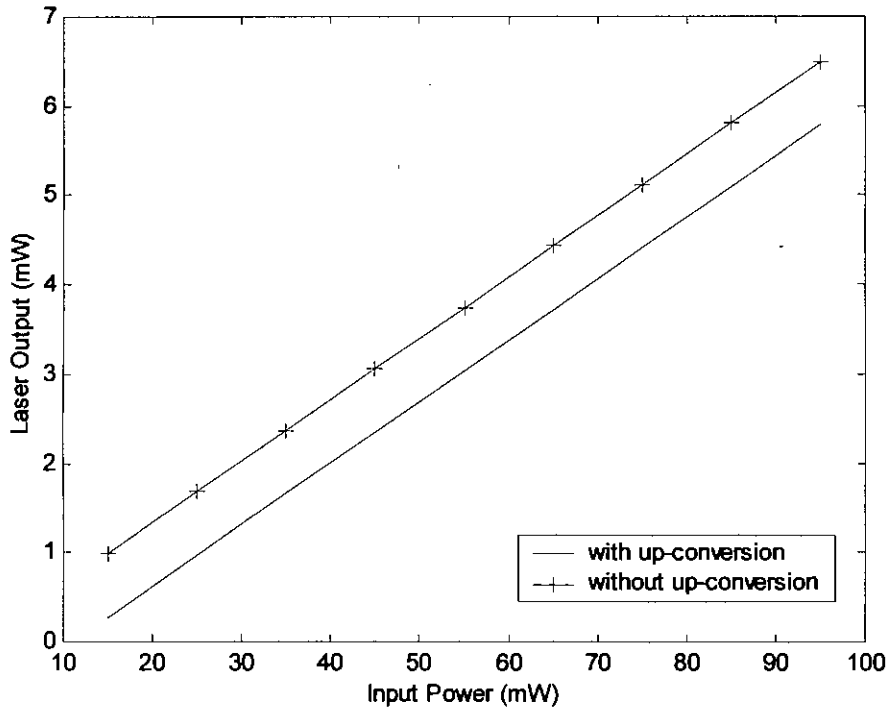
At small pump power, photons may be generated by spontaneous emission and only a small fraction of the spontaneous emission enters into lasing mode. Lasing starts above the threshold level at which optical gain compensates for all optical losses. Since stimulated emission is much higher as compared to spontaneous emission, from Fig 5.2 it is found that there is negligible amount of photon emission before threshold. Hence below threshold, ignoring the photon density  $N$  inside the cavity, we have calculated the value of carrier density at threshold,  $n_{si\_th}$  using Eq. (4.5.1). And above the threshold level, photon density hence laser output increases almost linearly with

pump power. Above threshold, both spontaneous and stimulated emission appears but spontaneous emission is extremely weak in relation to laser output as it is emitted in all directions and has a much greater frequency spread.



**Fig. 5.3** Calculated laser output profile under variable pump power to observe the effect of Auger process.

From Fig. 5.3 it is clear that there is no significant impact of Auger process on Er doped nc-Si laser output as Auger process provides a very small percentage (less than 1%) of the total non-radiative decay processes. This is due to the quantized nature of both the excitonic and the Er related levels [26]. Moreover it is considered that the optically active Er ions are located in SiO<sub>2</sub> or at the Si/SiO<sub>2</sub> interface, so Auger effect is suppressed due to the presence of oxide barrier layer between Er and nc-Si.



**Fig 5.4** Laser output as a function of pump power to observe the effect of cooperative up-conversion.

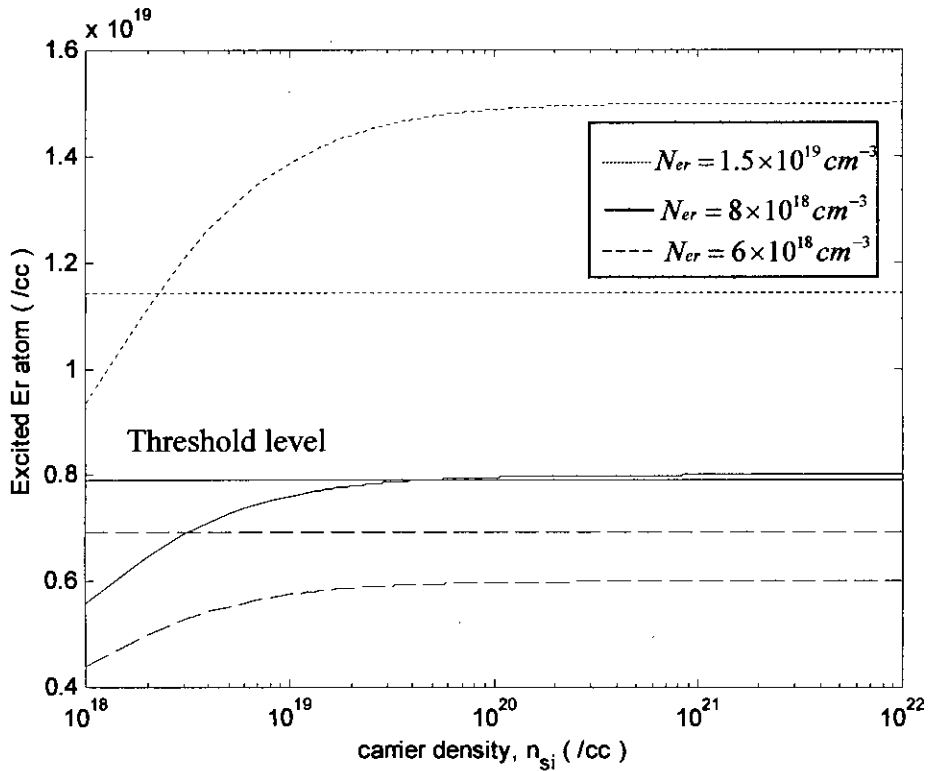
At high concentration, interaction between Er ions is an important gain limiting effect. Cooperative up-conversion is one such process in which excited Er ion de-excites by transferring its energy to a neighboring excited Er ion, promoting it into the  $^4I_{9/2}$  level. This effect lowers the output or conversely, increases the pump power needed to obtain a certain light output. Our observations also resemble these characteristics. This happens as the radiative efficiency decreases due to the increased non-radiative decay processes. In practice, cooperative up-conversion is an important gain limiting effect for Er concentrations above  $10^{19}$ - $10^{20}$  Er/cm<sup>3</sup>.

### 5.3 Effects of Different Parameters on Laser Operation

The lasing operation from erbium doped nanocrystal silicon is highly dependent on different parameters and proper design. In the next few sections we shall analyze the effects of some parameters on laser operation.

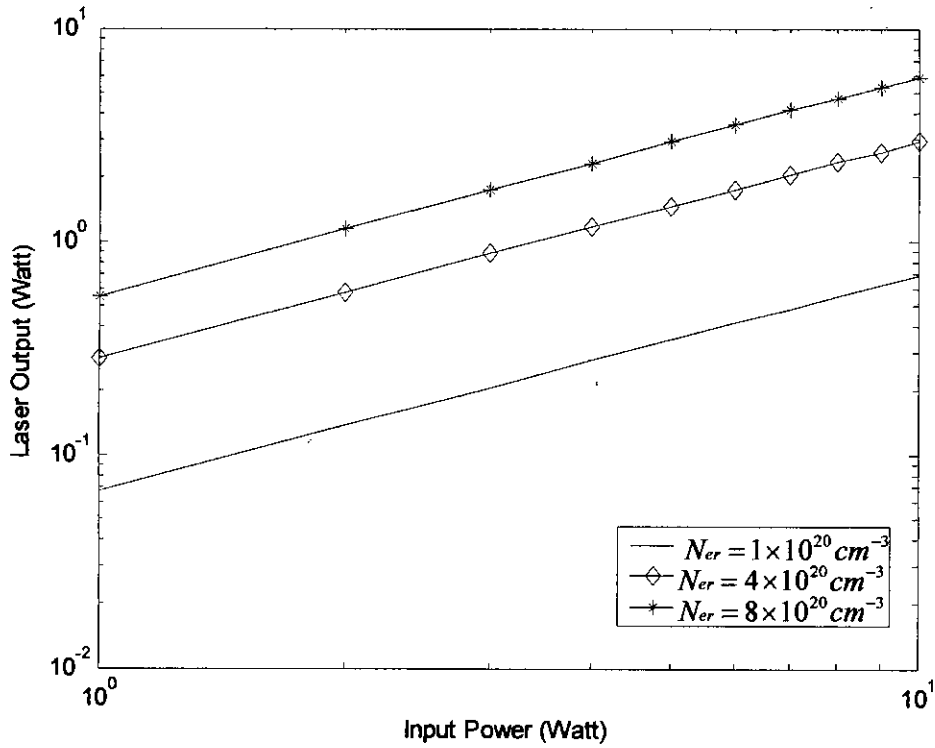


### 5.3.1 Effect of active Erbium concentrations ( $N_{er}$ )



**Fig. 5.5** Excited erbium atoms as a function of carrier density for different values active Er concentrations,  $N_{er}$ .

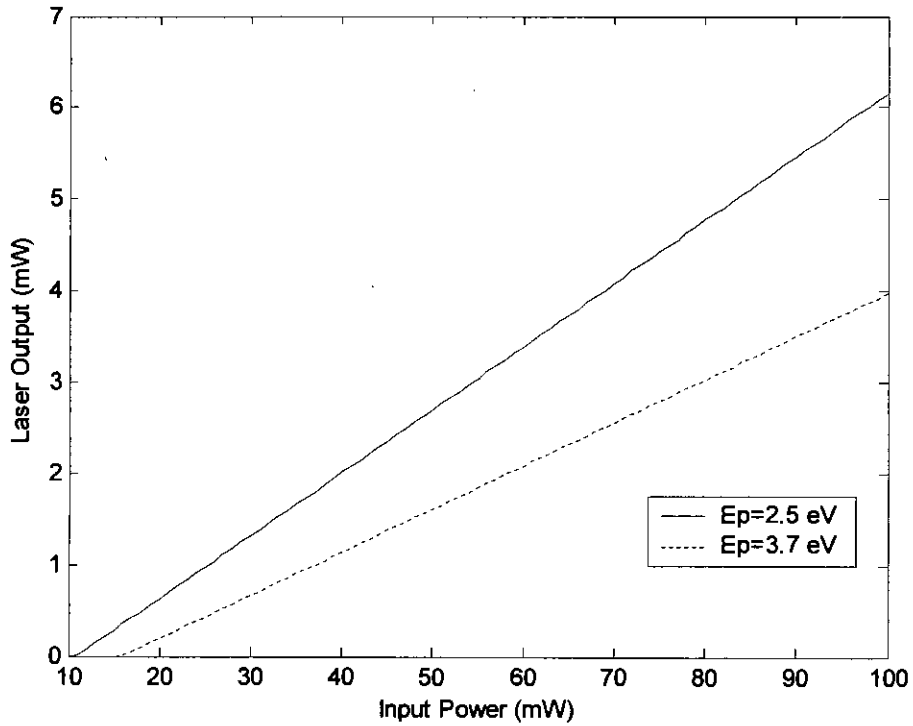
Fig. 5.5 shows the excited erbium atoms as a function of carrier density with no optical feedback. The amount of excited Er atom and the threshold level of population inversion for lasing condition changes with the change of erbium concentrations. It is found that the excited atoms can attain the respective threshold level required for the lasing operation upto a certain concentration level. In our analysis, lasing is possible with various levels of Er concentrations approximately upto  $N_{er} = 8 \times 10^{18} \text{ cm}^{-3}$ . But below this concentration level, lasing is not possible since excited atoms failed to attain the required threshold level.



**Fig. 5.6** Pump power dependence of the laser output at 1.54  $\mu\text{m}$  for nc-Si samples with different Er concentrations.

From Fig 5.6 it is found that for a fixed Er content, laser output increases linearly with pump power. Moreover, by increasing the Er content for a fixed pump power, the output at 1.54  $\mu\text{m}$  first increases proportionally to the Er concentration and, above a certain value, tends to saturate. This saturation phenomenon has shown experimentally by Franzo et al. [17]. It is due to the fact that, when the Er concentration increases, also the number of Er ions per nc-Si increases and therefore not all of them can be pumped by the same nanocrystal.

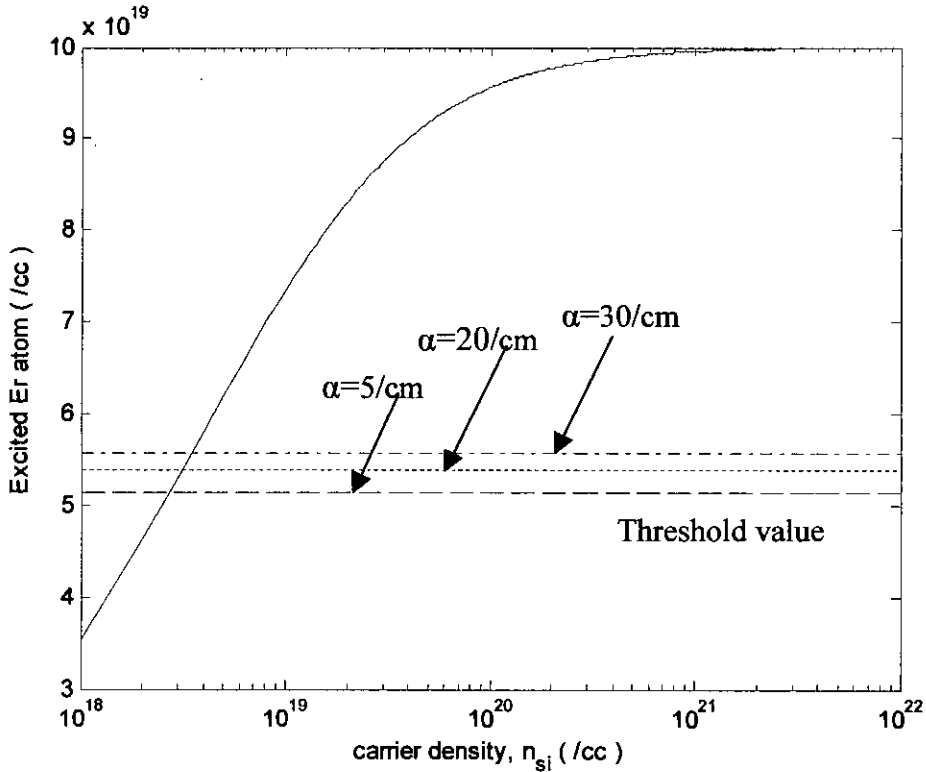
### 5.3.2 Effect of Optical Excitation Source



**Fig. 5.7** Calculated laser output profile under variable pumping with different energy optical sources.  $N_2$  laser ( $h\nu = 3.7$  eV) and Ar laser ( $h\nu = 2.5$  eV) have been used for optical excitation.

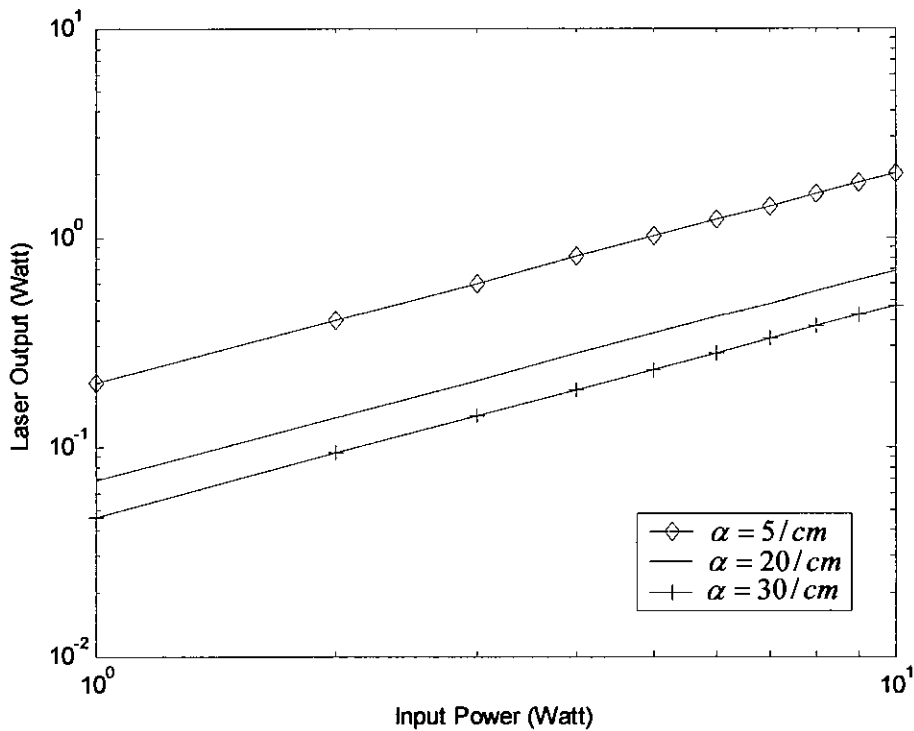
Fig. 5.7 shows the impact of photon energy on laser power. As pumping photon energy increases, for a certain pump power, the number of photogenerated excitons decreases. Hence the number of excited Er per nc-Si decreases which in turn decreases the Er luminescence. This also requires higher input power to achieve threshold excitation of erbium atom. The separation between two outputs increases with increasing pumping power. This is due to the fact that the difference between optical generations in these two cases increases linearly with pump power. Moreover in practice, at shorter wavelength, scattering loss of the cavity increases.

### 5.3.3 Effect of Internal Loss Coefficient ( $\alpha$ )



**Fig. 5.8** Excited erbium atoms as a function of carrier density for different values of loss co-efficient ( $\alpha$ ) with Er concentration of  $N_{er} = 10^{20} \text{ cm}^{-3}$ .

Fig. 5.8 shows the excited erbium atoms as a function of carrier density (solid line) with no optical feedback. The amount of excited Er atom remains same irrespective of the value of loss coefficient ( $\alpha$ ). With the change of loss coefficient, the threshold level of population inversion for lasing condition changes. For  $\alpha = 5 \text{ cm}^{-1}$ ,  $\alpha = 20 \text{ cm}^{-1}$  and  $\alpha = 30 \text{ cm}^{-1}$  the excited atoms can exceed the required threshold level for lasing operation. Hence for optimum values of loss coefficient, lasing is possible with Er concentration of  $10^{20} \text{ cm}^{-3}$ .

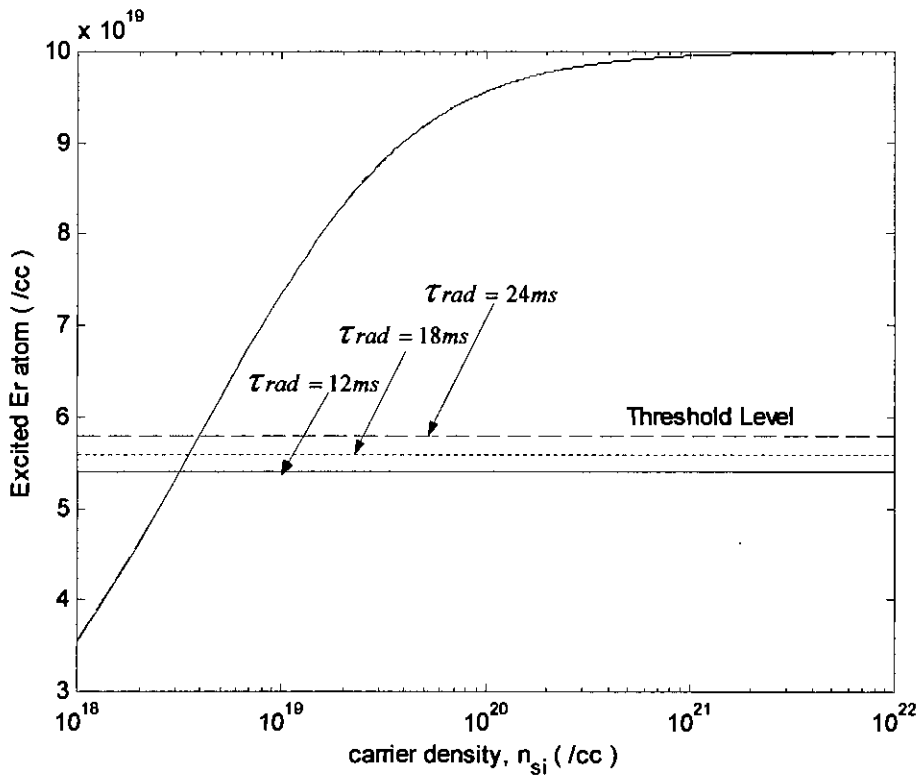


**Fig 5.9** Output power vs pump power of Er doped nc-Si laser for different values loss coefficient with  $N_{er} = 10^{20} \text{ cm}^{-3}$ .

Fig. 5.9 shows the effect of loss coefficient ( $\alpha$ ) on the output power. Higher value of  $\alpha$  causes lower laser output. When the pump power exceeds the threshold value, stimulated emission dominates the spontaneous emission and power output increases almost linearly with input power. Although the power above threshold is different at different  $\alpha$ , the spontaneous power is same. Because erbium excitation does not depend on  $\alpha$ . But with the increase of  $\alpha$ , threshold gain increases causing the more carrier to be needed for achieving the threshold excitation of erbium atom. So at higher value of  $\alpha$ , threshold pump power is also higher.

### 5.3.4 Effect of Er Radiative Lifetime ( $\tau_{rad}$ )

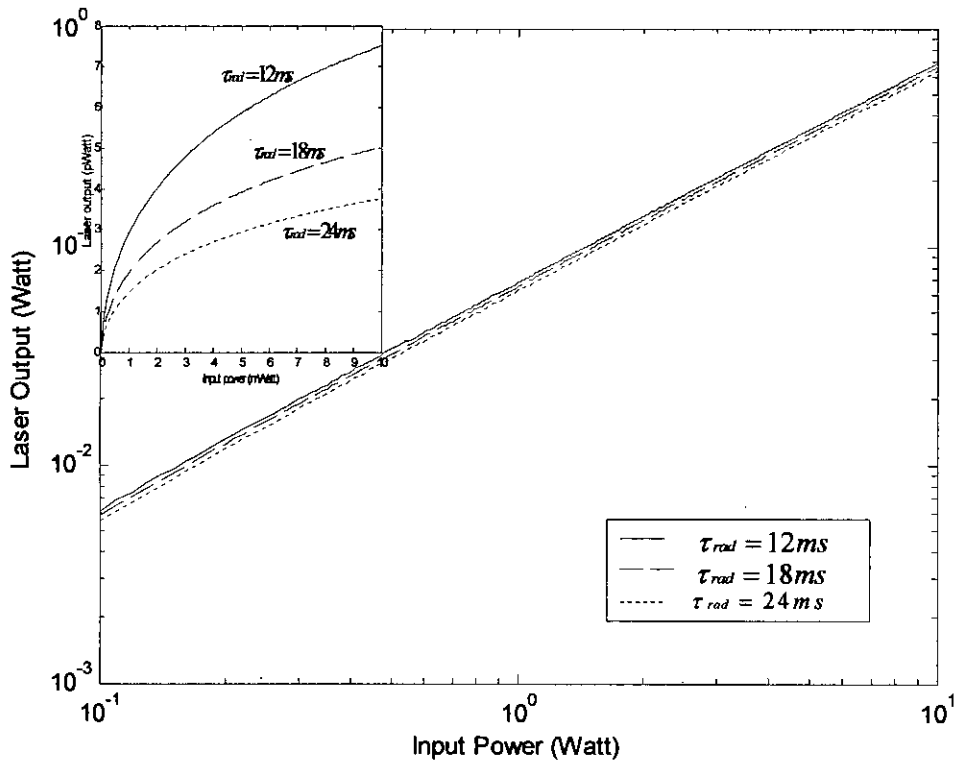
Fig. 5.10 shows the excited erbium atom for different radiative lifetime of erbium atom. The amount of excited erbium atoms remains same in three different cases but threshold level is different for different lifetime as before.



**Fig. 5.10** Excited erbium atom as a function of carrier density for different values of Er radiative lifetime with Er concentration of  $N_{er} = 10^{20} \text{ cm}^{-3}$ .

From this figure it is clear that for doping concentration of  $N_{er} = 10^{20} \text{ cm}^{-3}$ , it is possible to achieve the threshold level.

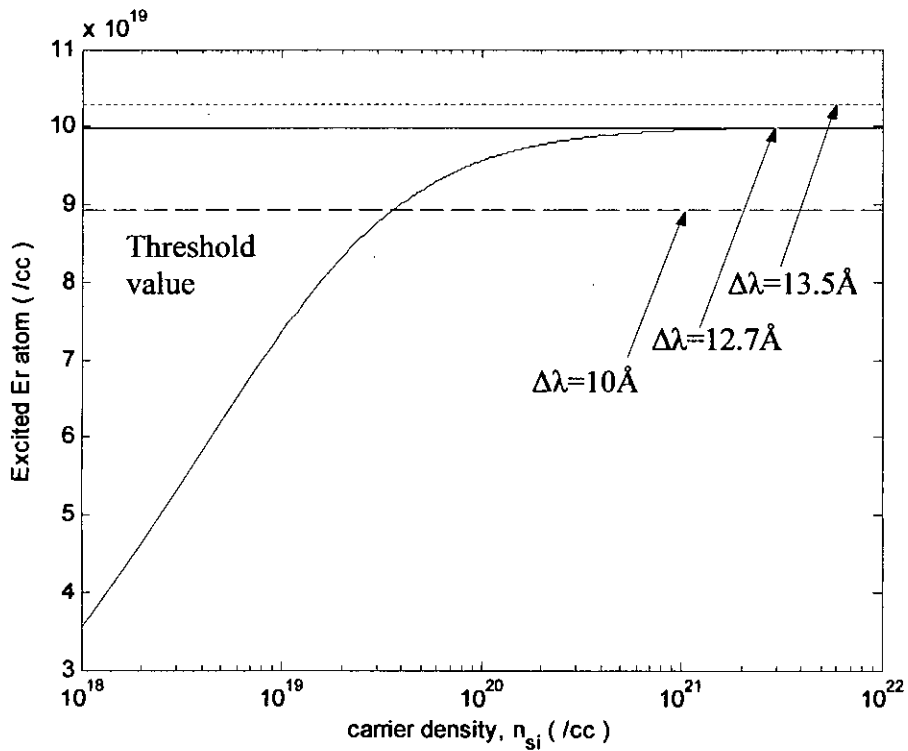
Fig. 5.11 shows the effect of radiative lifetime of erbium atom on laser output curve. From the figure, we cannot see any noticeable change in power output for different radiative lifetime, which implies that impact of radiative lifetime on laser output is negligible. Here below threshold, spontaneous power changes with the change of lifetime shown in the inset of Fig. 5.11. This is reasonable because spontaneous power is inversely proportional to the radiative lifetime.



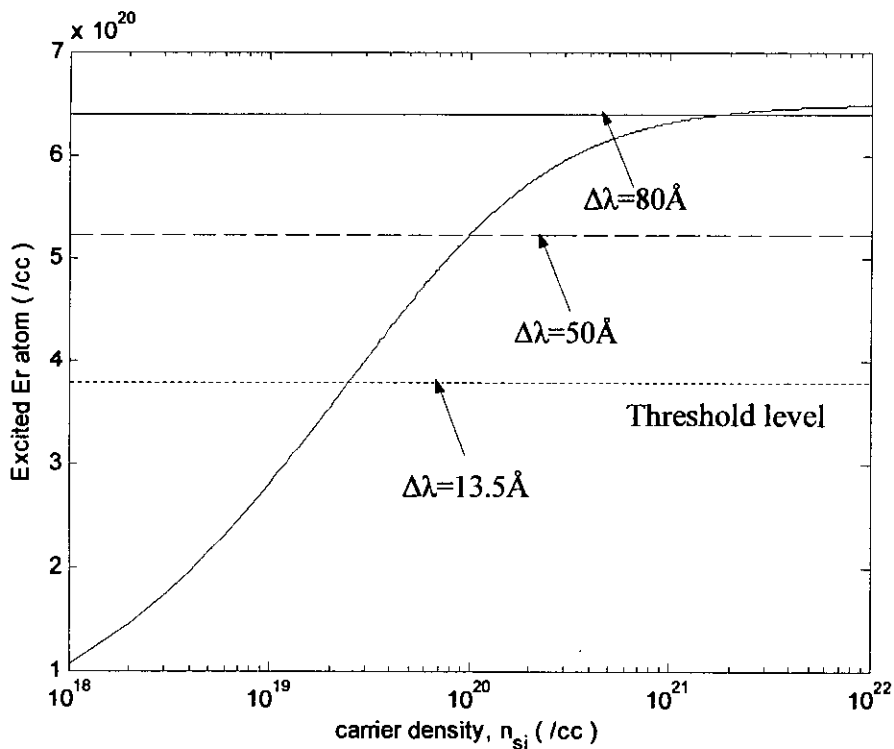
**Fig. 5.11** Laser output vs. pump power of Er doped nc-Si laser for different erbium radiative lifetime with Er concentration of  $N_{er} = 10^{20} \text{ cm}^{-3}$ . The inset shows only the spontaneous power.

### 5.3.5 Effect of Spectral Width ( $\Delta\lambda$ )

Fig. 5.12 and 5.13 shows the effect of spectral width on the Er atom excitation as a function of carrier density (solid line) with no optical feedback. The curve indicates that the Er atoms in the excited state do not change with changing the spectral width but the threshold level changes with different spectral width. When erbium concentration is  $N_{er} = 10^{20} \text{ cm}^{-3}$ , threshold can be achieved upto  $\Delta\lambda = 12.7 \text{ \AA}$ . But if the erbium concentration is increased to  $N_{er} = 6.5 \times 10^{20} \text{ cm}^{-3}$ , threshold is possible to achieve even at higher spectral width.

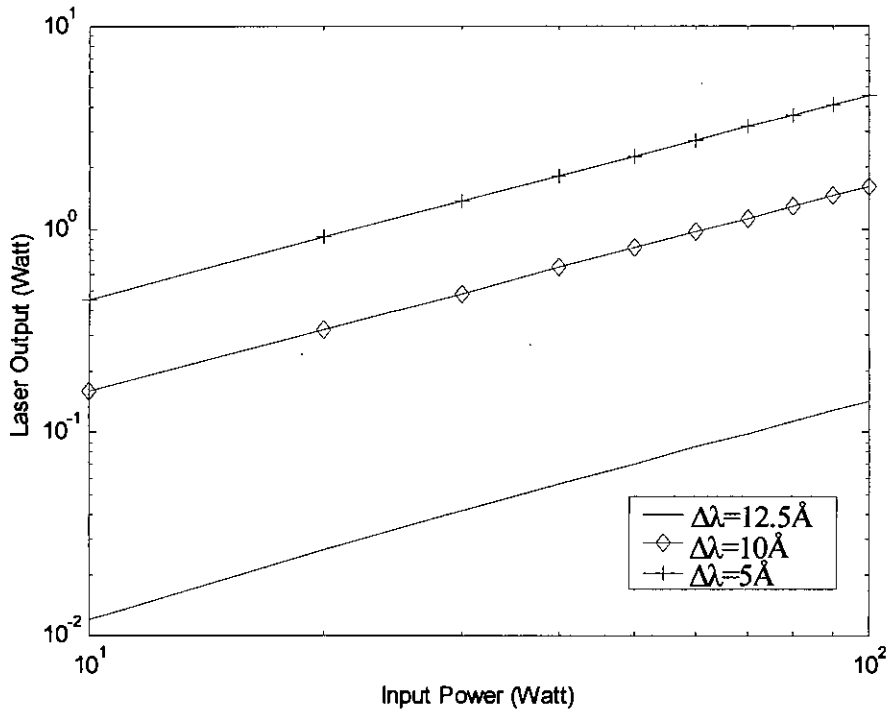


**Fig. 5.12** Excited erbium atom as a function of carrier density for different values of spectral width of emission with Er concentration of  $N_{er} = 10^{20} \text{ cm}^{-3}$ .



**Fig. 5.13** Excited erbium atom as a function of carrier density for different values of spectral width of emission with Er concentration of  $N_{er} = 6.5 \times 10^{20} \text{ cm}^{-3}$ .

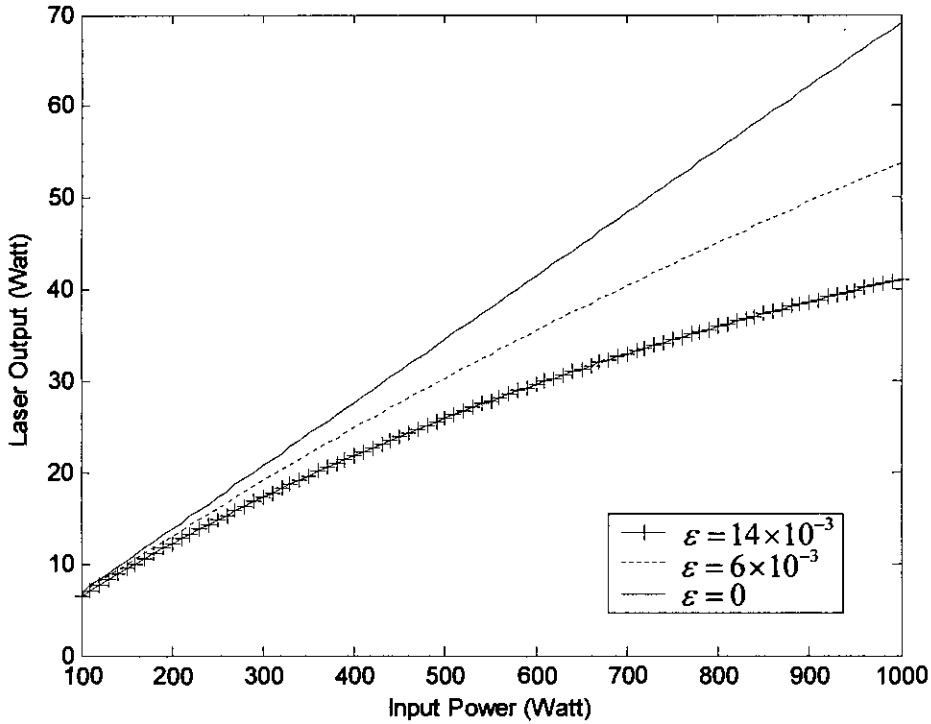




**Fig 5.14** Laser output vs. pump power of Er doped nc-Si laser for different spectral width of emission with Er concentration of  $N_{er} = 10^{20} \text{ cm}^{-3}$ .

Fig 5.14 shows the effect of spectral width of emission on laser output. With the increase of spectral width, the carrier density needed to establish a certain power output also increases. Hence laser output decreases with the increases of spectral width for a certain input power. Again, since the increased spectral width causes the threshold level to increase, this also increases the threshold pump power to achieve lasing condition.

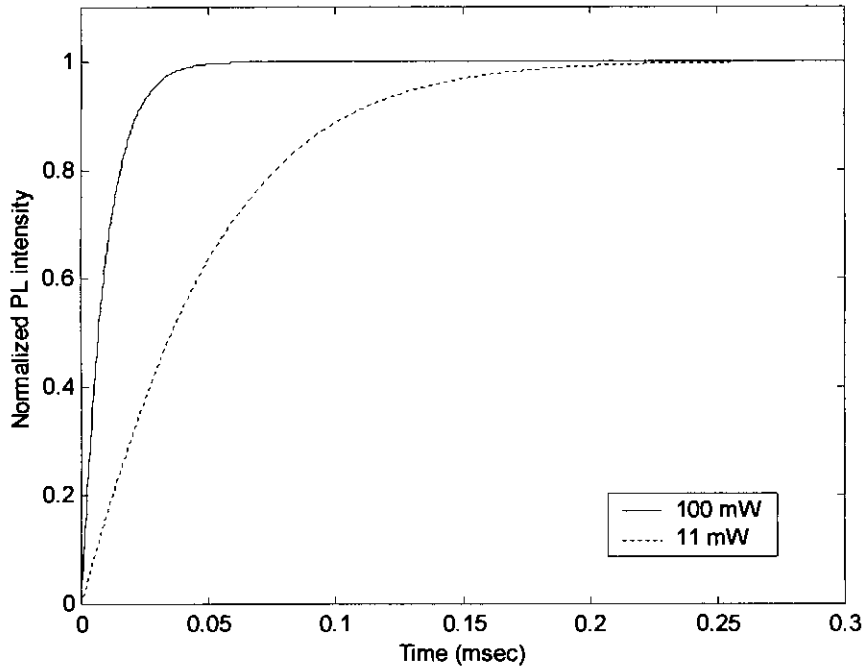
### 5.3.6 Effect of Input Dependent Loss Coefficient



**Fig. 5.15** Effect of input power dependent absorption loss coefficient on the Er doped nc-Si laser output power.

We have assumed that internal loss coefficient  $\alpha$  is constant irrespective of the carrier density. But practically, this value increases with the increase of carrier density. We have assumed that  $\alpha$  increases with input power like this  $\alpha = \alpha_0 + \epsilon Pin$ . Fig. 5.15 shows the effect of carrier dependent loss coefficient on laser output power. From figure, we see that output power is reduced as input power increases and tends to saturate. This effect is usually observed at high pump power.

## 5.4 Time dependent rise of Erbium luminescence

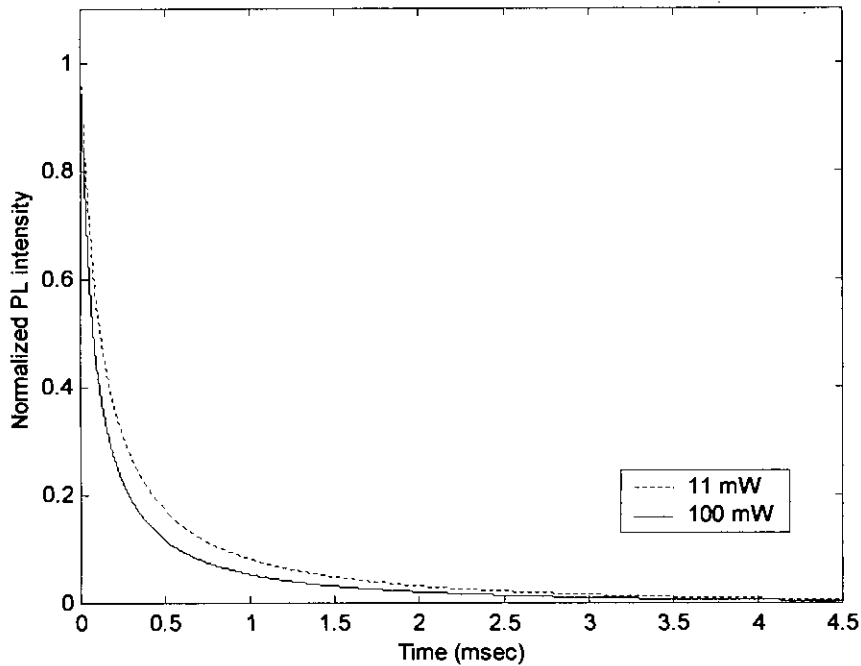


**Fig 5.16** PL intensity profile at two different excitation levels. Both the curves have been normalized to peak values.

Fig 5.16 shows that with the increase of excitation power, rise time (time required to establish luminescence from 10% to 90% of peak value) of photoluminescence (PL) decreases. This can be explained by the fact that at higher excitation level, increased carrier density increases Er excitation rate. This high carrier density also increases non-radiative decay processes but under constant excitation, radiative decay process dominates over non-radiative processes. Hence less time is required to establish a certain luminescence. Both the curves have been plotted (using Eq. 4.2.1) after normalizing to respective peak intensities.

## 5.5 Photoluminescence decay profile

Fig 5.17 shows two PL decay profiles at two different excitation levels. Here also the curves have been plotted (using Eq. 4.3.1) after normalizing to respective peak intensities. The figure shows that increasing excitation power increases PL decay rate.

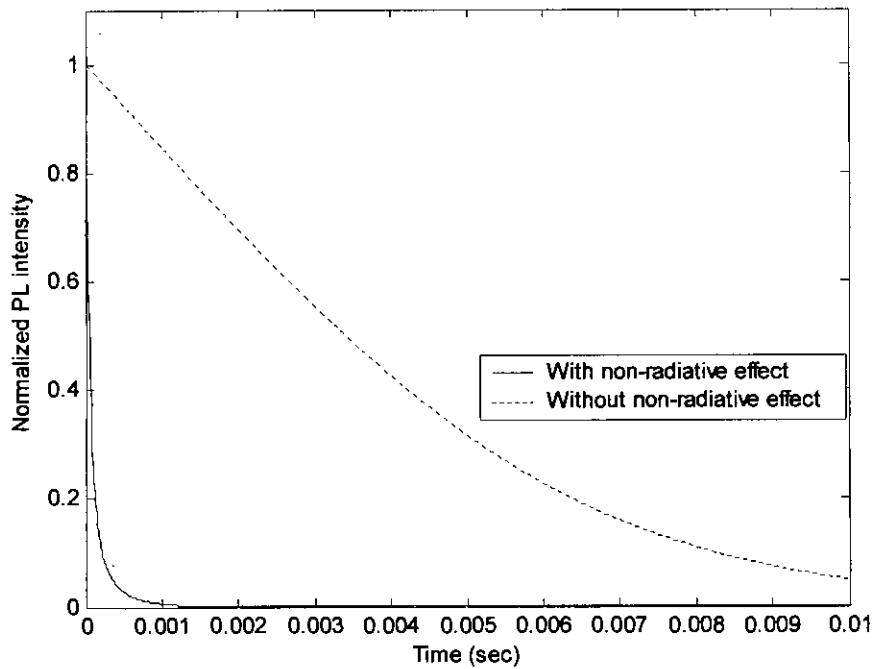


**Fig 5.17** PL decay profile at two different excitation levels. Both the curves have been normalized to peak values.

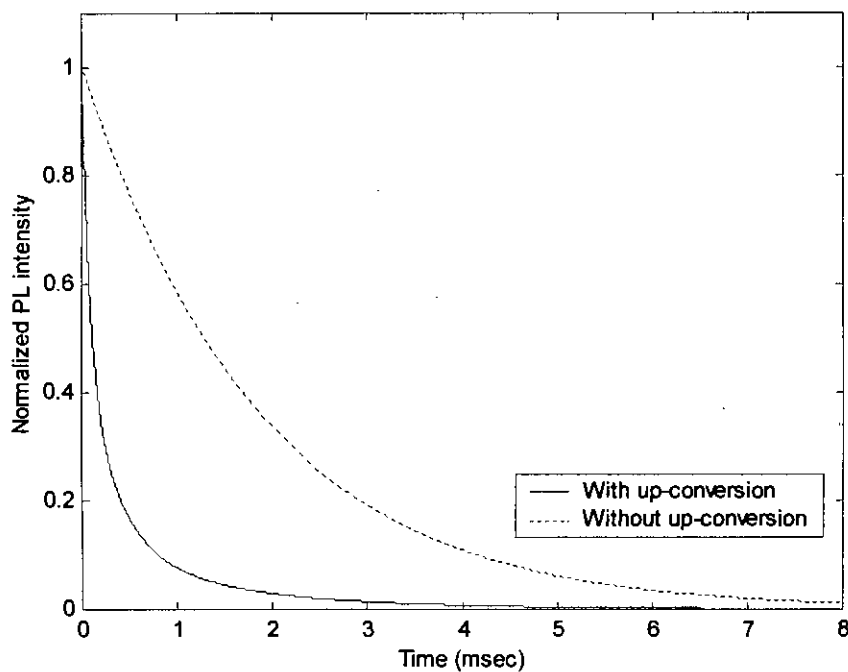
This effect has been experimentally found by Pacifici et al. [26]. With increasing excitation power, the carrier density increases which in turn increase non-radiative decay processes. Once the excitation is switched off, these non-radiative decay processes dominate and cause a fast decay of photoluminescence. The impact of non-radiative decay processes on PL decay is shown in Fig 5.18. Cooperative up-conversion effect, among the non-radiative processes, plays the dominant role in decay profile. These effects are shown in Fig 5.19 and Fig 5.20.

If we define time constant as the time to reach  $1/e$  or 36.8% of the peak value, we can also see that the time constant for higher excitation power is lower than that for lower excitation power.

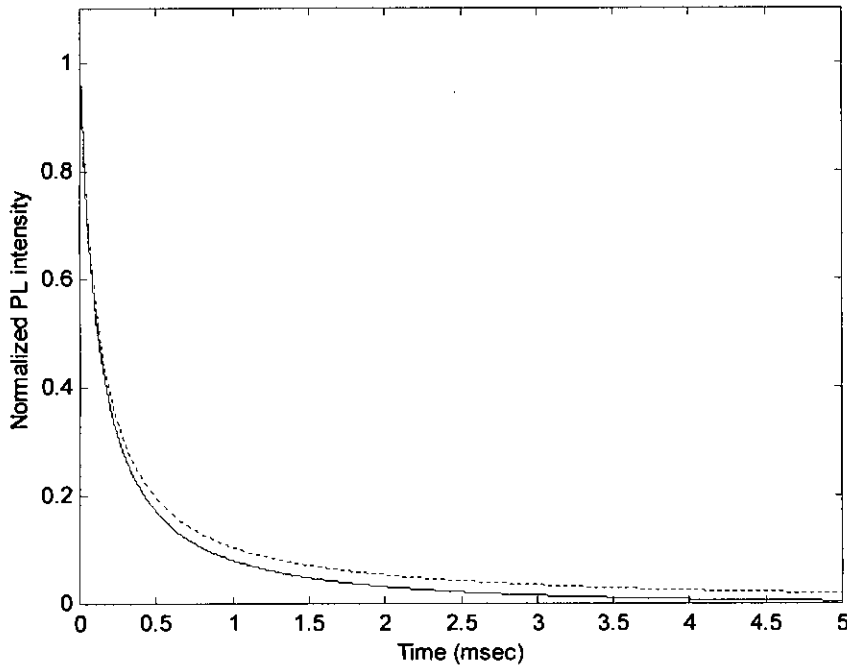
Fast response is always desirable since fast switching is a key point in high speed optoelectronic devices.



**Fig 5.18** PL intensity profile at 11mW excitation power under two different conditions. Both the curves have been normalized to peak values.



**Fig 5.19** PL intensity profile at 11mW excitation power to observe the impact of cooperative up-conversion effect on PL decay profile while other processes exist in both cases. Both the curves have been normalized to respective peak values.

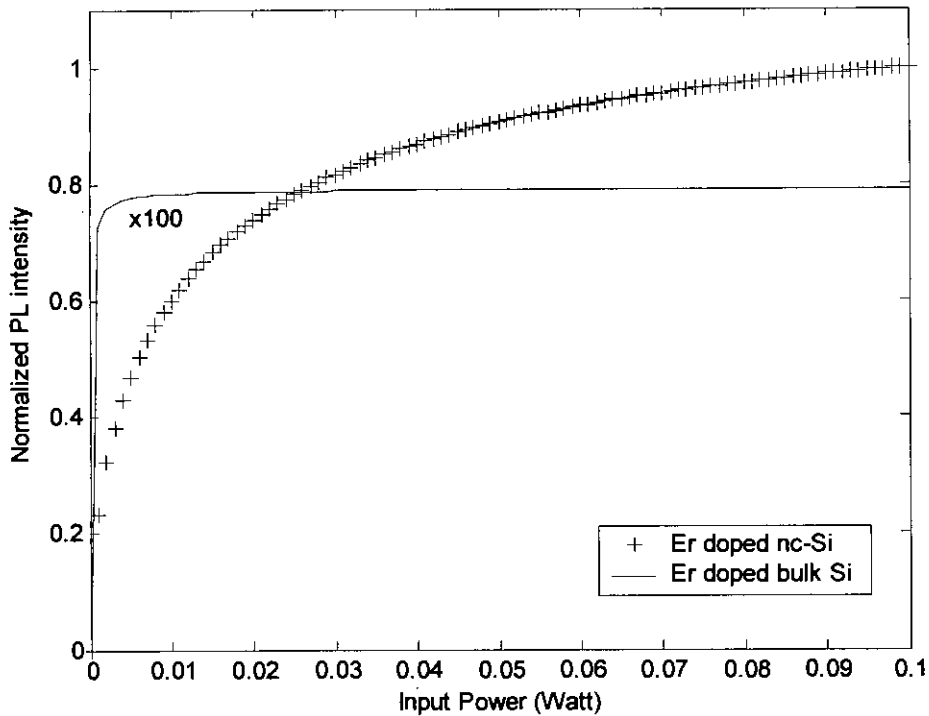


**Fig 5.20** PL intensity profile at 11mW excitation power to observe the impact of non-radiative processes, except cooperative up-conversion effect, on PL decay profile. The solid line curve shows the decay profile after the inclusion of other non-radiative processes. Both the curves have been normalized to respective peak values.

## 5.6 Er doped Bulk Silicon and Nanocrystal Silicon

### Luminescence from Erbium ions

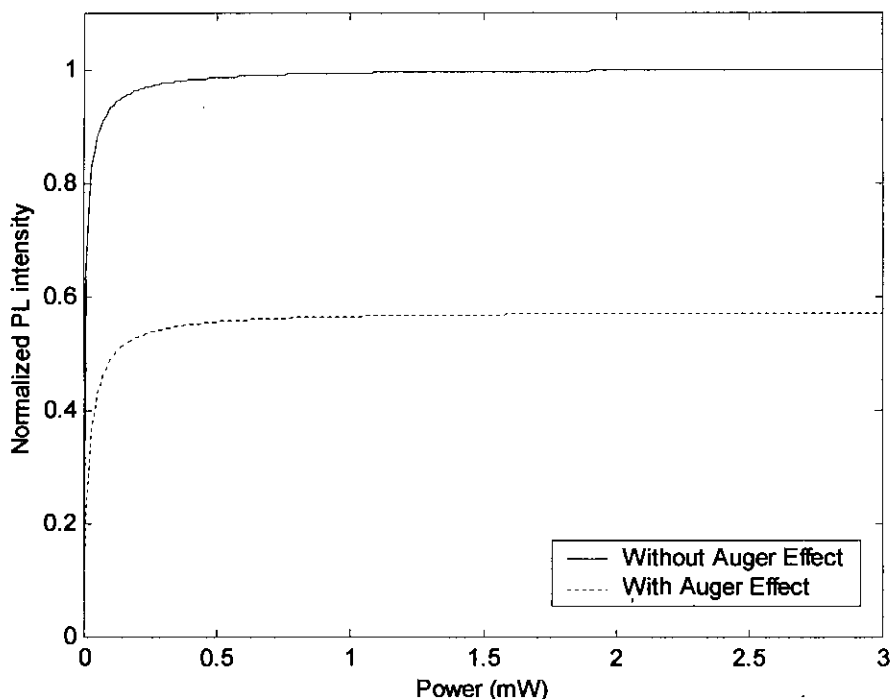
The electronic structure of silicon nanocrystal is strongly modified from that of bulk Si crystals due to the confinement of electrons and holes in a space smaller than the exciton Bohr radius of bulk Si crystal. The modification of the electronic structure provides nc-Si with functions which do not occur in bulk Si crystals. In nc-Si, erbium ions can be excited very efficiently by the energy transfer from nanocrystal; the effective absorption cross section of the intra-4f shell transition of  $\text{Er}^{3+}$  is



**Fig 5.21** Photoluminescence Intensity of Er vs. pump power profile. Typical values of different parameters have been used [luminescence from Er:bulk Si system is multiplied by 100].

enhanced by 2-4 orders of magnitude because of the large absorption cross section of nc-Si and because of the efficient energy transfer from nc-Si to  $\text{Er}^{3+}$  [15]. These effects highly enhance the luminescence from Er in nc-Si. Moreover, the non-radiative de-excitation processes typically limiting Er luminescence in bulk Si, namely, Auger process and energy back transfer, are strongly reduced in this case further improving the luminescence yield. Fig 5.21 shows the luminescence from Er in nanocrystal and bulk silicon [38]. From figure it is clear that the erbium luminescence from nc-Si is much higher than that from bulk Si. Similar phenomena are also experimentally shown by Franzo et al. [17]. Like bulk silicon, the saturation of PL intensity at higher excitation power has been also observed in nc-Si because the amount of the energy transferred to  $\text{Er}^{3+}$  is limited by the number of  $\text{Er}^{3+}$ . This saturation phenomenon has been shown experimentally by Fujii et al. [18].

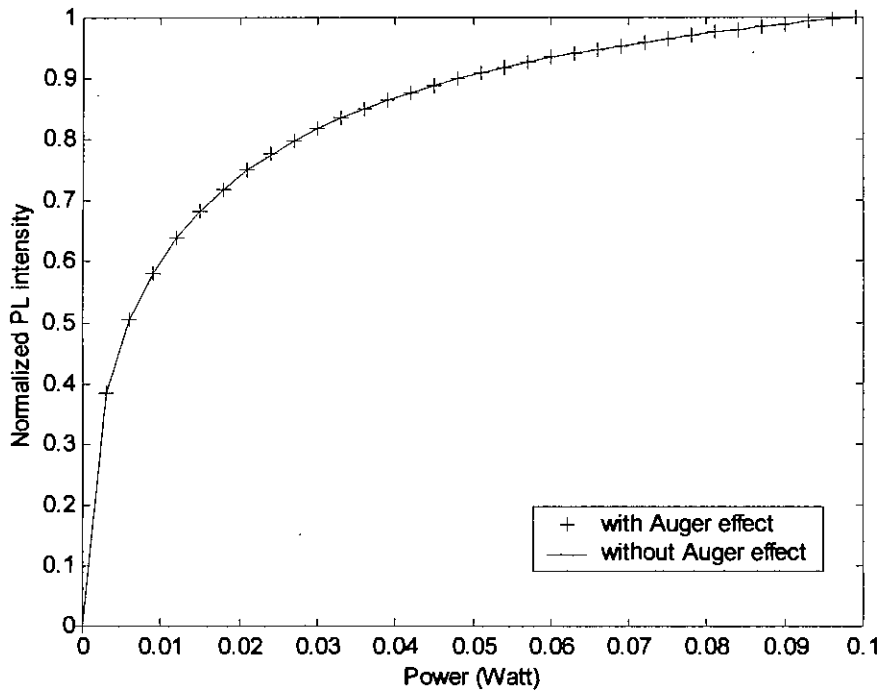
## Effect of Auger Process



**Fig 5.22** Calculated PL intensity profile from Erbium doped bulk Silicon under variable photo-excitation. Typical values of different parameters have been used.

The impurity Auger effect in Er doped bulk silicon, where the energy of an excited level of Er can be given up to a carrier (electron or hole) which is free in the conduction or valence band of bulk Si, promoting it to a higher lying level plays a dominant role in non-radiative decay processes of Er in Si. Fig 5.22 shows the result of inclusion of Auger effect at very low temperature (9 K) [38]. The inclusion of Auger effect causes an increase in non-radiative Er decay rate, which is responsible for the reduced PL intensity. On the other hand, as discussed earlier, the effect Auger process on Er luminescence in nc-Si is negligible as compared to other non-radiative decay process. Fig 5.23 shows the impact of Auger process in Er doped nc-Si. It is also explained by Pacifici et. al. [26] that due to the quantized nature, the Auger effect with nanocrystal should be less efficient than in bulk Si.





**Fig 5.23** Calculated PL intensity profile from Erbium doped nc-Si under variable photo-excitation.

A drawback to use a bulk silicon crystal as a host of  $\text{Er}^{3+}$  is the large temperature quenching of the  $1.54 \mu\text{m}$  luminescence. The temperature quenching arises from the dissociation of an electron-hole pair bound to the Er related level before the energy is transferred to  $\text{Er}^{3+}$  and the de-excitation of an excited  $\text{Er}^{3+}$  by forming an electron-hole pair at the Er related level (energy back transfer) [28]. Energy back transfer is a phonon assisted process. But using Si nanocrystals as a host of Er can drastically reduce this temperature quenching [28]. The band gap widening of nc-Si arising from the confinement of an electron-hole pair in a small volume (quantum size effects) is considered to be responsible for the observed negligible temperature quenching. Because the energy mismatch between Er and nc-Si related levels is too great to be made up by phonon interactions. Moreover, since optically active erbium ions lie outside the silicon nanocrystals, energy back transfer is suppressed due to presence of an oxide barrier layer between the erbium and the nanocrystal.

Again, it is found that nanocrystal decay rate increases with increasing temperature. But the Er luminescence is constant upto room temperature implies that the energy transfer from nanocrystal to Er must occur well within the nanocrystal decay time at room temperature. Consequently, energy transfer rate constant must be large enough. This constant Er luminescence is experimentally obtained by Kik et al. [21] and Priolo et al. [22].

# Chapter Six

## Conclusion

### 6.1 Conclusion

Interests in photoluminescence from the erbium ions,  $\text{Er}^{3+}$  in silicon matrices can be traced to the need to develop silicon optoelectronic devices capable of operating at a wavelength of  $1.54 \mu\text{m}$  due to the internal 4f-shell transition ( ${}^4\text{I}_{13/2} - {}^4\text{I}_{15/2}$ ) of Er ions, which falls at the minimum of absorption in fiber-optic communication lines. In this thesis, a mathematical model for the erbium excitation and de-excitation processes in silicon nanocrystals embedded in  $\text{SiO}_2$  has been developed. Optical properties of erbium and its effect in bulk and nanocrystal silicon have been studied. The excitation mechanism of erbium through recombination of excitons confined in nc-Si has been analyzed for conditions of achieving the lasing threshold. The sample (Er: nc-Si) has been excited through optical sources. Exponential decay of light within the system has been considered for the overall optical losses. An optical cavity has been designed which provides sufficient optical gain to overcome losses and provides emission of coherent light. Rate equations involving erbium excitation, photon generation and decay etc. has been solved and an estimation of the output power of the proposed laser device has been made. The dependency of laser output on different parameters has been studied and good agreement with the characteristics of typical laser has been achieved. Enhancement of the absorption coefficient of light with the increase of input has also been incorporated. Time dependent luminescence and decay profile of Er incorporated nc-Si have been made. Also a comparison between Er: nc-Si and Er: bulk Si under different conditions has been studied.

### 6.2 Recommendation for future work

The electronic structure of nc-Si changes continuously from the bulk structure with decreasing size. As a result, the optical property of nc-Si is small modifications of those of bulk Si crystals and all parameters (e.g. band gap energy, exciton lifetime, degree of electron-hole exchange interaction, and so on) change continuously from

bulk values. In our analysis, we have incorporated some characteristics but a number of other quantum effects can be investigated. Hence, there remains a scope of extensive research in this field. The impact of preparation procedure of nanocrystal silicon, annealing temperature etc. may be another field of research.

We have performed steady state analysis of laser from Er doped nc-Si. The dynamic characteristics of laser, modulation techniques and frequency response of laser and LED are unexplored. A research may be carried out in these fields. Comparative study between laser and LED in integrated system design may be made.

Transmission and detection of optical signal is essential in optoelectronic systems. So nanometer sized silicon based waveguide and detectors may be another topic of research.  $\text{Er}^{3+}$  ions incorporated into Si produce stable sharp luminescence at around 1.54  $\mu\text{m}$  wavelength which corresponds to the absorption minimum in silica-based glass fibers. It may be proved very effective in fiber optic communication line if nc-Si can be incorporated in the EDF because in this case fiber optic, itself acts as cavity. So research may be carried out in this field.

We see from fig 5.16 and fig. 5.17 that PL intensity takes comparatively longer time to become steady i.e. rise time and decay time are comparatively high. This phenomenon is a great hurdle in high frequency optoelectronic operation. Since high speed information system requires a quick responding device. Future research effort may be concentrated in this field.

# Bibliography

- [1] D. G. Hall, in *Silicon-Based Optoelectronic Materials*, edited by M.A. Tishler, R.T. Collins, M. L. W. Thewalt and G. Abstreiter [Mat. Res. Soc. Symp. Proc. 298, 367 (1993)].
- [2] H. Ennen, J. Schneider, G. Pomrenke and A. Axmann, *Appl. Phys. Lett.*, Vol. 43, p. 943, 1983.
- [3] P. B. Klein and G. H. Pomrenke, *Electr. Lett.* 24, p. 1502, 1988.
- [4] H. Ennen, J. Wagner, H. D. Müller and R. S. Smith, *J. Appl. Phys.*, Vol. 61, p. 4877, 1987.
- [5] Y. S. Tang, K. C. Heasman, W. P. Gillin and B. J. Sealy, *Appl. Phys. Lett.*, Vol. 55, p. 432, 1989.
- [6] J. Michel, J. L. Benton, R. F. Farante, D. C. Jacobson, D. J. Eaglesham, E. A. Fitzgerald, Y. H. Xie, J. M. Poate and L. C. Kimerling, *J. Appl. Phys.*, Vol. 70, p. 2672, 1991.
- [7] D. L. Alder, D. C. Jacobson, D. J. Eaglesham, M. A. Marcus, J. L. Benton, J. M. Poate and P. H. Citrin, *Appl. Phys. Lett.*, Vol. 61, p. 2181, 1992.
- [8] S. Libertino, S. Coffa, G. Franzo and F. Priolio, "The effects of oxizen and defects on the deep level properties of Er in crystalline Si," *Appl. Phys. Lett.*, Vol. 78, p. 3867, 1995.
- [9] S. Coffa, G. Franzo, F. Priolio, A. Polman and R. Serna, "Temperature dependence and quenching processes of the intra-4f luminescence of Er in crystalline Si," *Phys. Rev. B*, Vol. 49, p. 16313, 1993.
- [10] F. Priolo, G. Franzo, S. Coffa, A. Polman, S. Libertino, R. Barklie and D. Carey, "The erbium-impurity interaction and its effect on the 1.54 m Luminescence of Er<sup>3+</sup> in crystalline silicon," *Appl. Phys. Lett.*, Vol. 78, p. 3874, 1995.
- [11] P. G. Kik, M. J. A. De Dood, K. KiKoin and A. Polman, "Excitation and deexcitation of Er<sup>3+</sup> in crystalline silicon," *Appl. Phys. Lett.*, Vol. 70, p. 1721, 1997.

- [12] F. Priolo, G. Franzo, S. Coffa, and A. Carnera, "Excitation and non-radiative de-excitation processes of  $\text{Er}^{3+}$  in crystalline Si," *Phys. Rev. B*, Vol. 57, p. 4443, 1998.
- [13] J. Palm, F. Gan, B. Zheng, J. Michel and L. C. Kimerling, "Electroluminescence of erbium-doped silicon," *Phys. Rev. B*, Vol. 54, p. 17603, 1996.
- [14] G. Franzo, F. Priolo, S. Coffa, A. Polman and A. Carnera, "Room-temperature electroluminescence from Er-doped crystalline Si," *Appl. Phys. Lett.*, Vol. 64, p. 2235, 1994.
- [15] M. Fujii, K. Imakita, K. Watanabe and S. Hayashi, "Coexistence of two different energy transfer processes in  $\text{SiO}_2$  films containing Si nanocrystals and Er", *J. Appl. Phys.*, vol. 95, no. 1, pp. 272-280, 1 January, 2004.
- [16] A. C. S. Samia, Y. Lou, C. Burda, R. A. Senter and J. L. Coffey, "Effect of the erbium dopant architecture on the femtosecond relaxation dynamics of silicon nanocrystals", *J. of Chemical Physics*, vol. 120, no. 18, pp. 8716-8723, 8 May, 2004.
- [17] Giorgia Franzo, Domenico Pacifici, Vincenzo Vinciguerra, Francesco Priolo and Fabio Lacona, " $\text{Er}^{3+}$  ions-Si nanocrystals interactions and their effects on the luminescence properties", *Appl. Phys. Lett.*, vol. 76, no. 16, pp. 2167-2169, 17 April, 2000.
- [18] M. Fujii, M. Yoshida, Y. Kanzawa, S. Hayashi and K. Yamamoto, "1.54  $\mu\text{m}$  photoluminescence of  $\text{Er}^{3+}$  doped into  $\text{SiO}_2$  films containing Si nanocrystals: Evidence for energy transfer from Si nanocrystals to  $\text{Er}^{3+}$ ", *American Institute of Physics*, 71 (9), pp. 1198-1200, 1 September, 1997.
- [19] P. G. Kik and A. Polman, "Exciton-erbium interactions in Si nanocrystal-doped  $\text{SiO}_2$ ," *J. Appl. Phys.*, Vol. 88, no. 4, pp. 1992-1998, 15 August, 2000.
- [20] A. J. Kenyon, S. S. Bhamber and C. W. Pitt, "The infra-red photoresponse of erbium-doped silicon nanocrystals," *Material Science and Engineering*, vol. B105, pp. 230-235, 2003.
- [21] P.G. Kik, M.L. Brongersma and A. Polman "Strong exciton-erbium coupling in Si nanocrystal-doped  $\text{SiO}_2$ ", *Appl. Phys. Lett.*, vol. 76, no. 17, pp. 2325-2327, 24 April, 2000.

- [22] F. Priolo, G. Franzo, F. Iacona, D. Pacifici, V. Vinciguerra, *Material Science and Engineering*, B81, 9 (2001)
- [23] V. Yu. Timoshenko, O. A. Shalygina, M. G. Lisachenko, D. M. Zhigunov, S. A. Teterrukov, P. K. Kashkarov, D. Kovalev, M. Zacharias, K. Imakita and M. Fujii, "Erbium ion luminescence of silicon nanocrystal layers in a silicon dioxide matrix measured under strong optical excitation", *Physics of the Solid State*, vol. 47, no. 1, pp. 121-124, 2005.
- [24] J. Lee, J. Shin and N. Park, "Optical Gain at 1.54  $\mu\text{m}$  in Nanocrystal Si-Sensitized Er-Doped Silica Waveguide Using Top-Pumping 470 nm LEDs," *J. of Lightwave Technol*, Vol. 23, p. 19, 2005.
- [25] J. Heitmann, M. Schmidt, M. Zacharias, V. Yu. Timoshenko, M. G. Lisachenko and P. K. Kashkarov, "Fabrication and photoluminescence properties of erbium doped size controlled silicon nanocrystals", *Material Science and Engineering*, vol. B105, pp. 214-220, 2001.
- [26] D. Pacifici, G. Franzo, F. Priolo, F. Iacona, L. D. Negro, "Modeling and perspectives of the Si nanocrystals-Er interaction for optical amplification," *Phys. Rev. B*, Vol. 67, p. 245301, 2003.
- [27] Fabio Iacona, Giorgia Franzo, Eduardo Ceretta Moreira and Francesco Priolo, "Silicon nanocrystals and  $\text{Er}^{3+}$  ions in an optical microcavity", *J. Appl. Phys.*, vol. 89, no. 12, pp. 8354-8356, 15 June, 2001.
- [28] K. Watanabe, M. Fujii and S. Hayashi, "Resonant excitation of  $\text{Er}^{3+}$  by the energy transfer from Si nanocrystals," *J. Appl. Phys.*, vol. 90, no. 9, pp. 4761-4767, 1 November, 2001.
- [29] S. Hufner, *Optical spectra of transparent rare earth compounds*, Academic, New York, 1978.
- [30] Y. H. Xie, E. A. Fitzgerald and Y. J. Mil, "Evaluation of erbium-doped silicon for optoelectronic applications," *J. Appl. Phys.*, Vol. 70, p. 3223, 1991.
- [31] D. T. X. Thao, C. A. J. Ammerlaan and T. Gregorkiewicz, "Photoluminescence of erbium-doped silicon: Excitation power and temperature dependence", *J. Appl. Phys.*, vol. 88, no. 3, pp. 1443-1455, 1 August, 2000.

- [32] M. Q. Huda and S. I. Ali, "A study on stimulated emission from erbium in silicon", *Material Science and Engineering*, vol. B105, pp. 146-149, 2003.
- [33] D. Pacifici, G. Franzo, F. Iacona, Boninelli, A. Irrera, M. Miritello and F. Priolo, "Er doped Si nanostructures", *Material Science and Engineering*, vol. B105, pp. 197-204, 2003.
- [34] I. N. Yassievich and A. S. Moskalenko, "Excitation mechanism of erbium photoluminescence in bulk silicon and silicon nanostructures," *Material Science and Engineering*, vol. B105, pp. 192-196, 2003.
- [35] P. M. Fauchet, J. Ruan, H. Chen, L. Pavesi, L. Dal Negro, M. Cazzanelli, R. G. Elliman, N. Smith, M. Sanoc and B. Luther-Davies, "Optical gain in Different silicon nanocrystal systems," *Optical Materials* 27, pp. 745-749, 2005.
- [36] J. Wilson and J. F. B. Hawkes, *Optoelectronics An Introduction*, Second edition, Prentice-Hall International (UK) Limited, 1996.
- [37] Shun Lien Chuang, *Physics of Optoelectronic Devices*, Second edition, John Willy & Sons, New York, 1995.
- [38] S. I. Ali, *Modeling of Spontaneous and Stimulated emission of Erbium in Silicon*, M.Sc. Thesis, Dept. of EEE, BUET, 2002 ✓





# APPENDIX – A

Flowchart for calculation of Photolumumescence decay profile of Er atom in nanocrystal Silicon

